

# 國立交通大學

電子工程學系電子研究所碩士班

碩士論文

行走區域標示及危險狀況判別之

盲人輔助系統

**Walking Area Labeling and Dangerous  
Situation Detection for Visually Impaired**



研究生：鄭綱

指導教授：王聖智博士

中華民國一〇〇年九月

行走區域標示及危險狀況判別之  
盲人輔助系統

**Walking Area Labeling and Dangerous Situation Detection  
for Visually Impaired**

研究生：鄭綱

Student：Kang Cheng

指導教授：王聖智博士

Advisor：Dr. Sheng-Jyh Wang



Submitted to Department of Electronics Engineering & Institute of Electronics

College of Electrical and Computer Engineering

National Chiao Tung University

in partial Fulfillment of the Requirements

for the Degree of Master

in

Electronics Engineering

September 2011

Hsinchu, Taiwan, Republic of China

中華民國一〇〇年九月

# 行走區域標示及危險狀況判別之 盲人輔助系統

研究生：鄭綱

指導教授：王聖智博士

國立交通大學

電子工程學系電子研究所碩士班



在本論文中，我們提出一套以視覺為基礎的盲人輔助系統。本系統採用了資料庫為主的架構，首先具有正常視力之輔助者事先於盲人經常行走之區域，建立 360 度全景之資料庫，並對資料庫圖片事前標籤重要的物體，像是人行道及道路；然後從全景資料庫中尋找與使用者前方視野最相近的區域；接著把此最接近之區域的標籤利用兩張影像之間的對應，產生目前環境的標籤；最後利用推論的標籤來判斷盲人目前的處境是否危險。只要使用者處於有設置資料庫的環境下，本系統能幫助盲人辨識可行走的區域，達成輔助盲人安全行走之目標。

# Walking Area Labeling and Danger Detection for Visually Impaired

Student: Kang Cheng

Advisor: Dr. Sheng-Jyh Wang

Department of Electronics Engineering, Institute of Electronics  
National Chiao Tung University

## Abstract

In this thesis, we propose a data-driven system that assists blind people to walk safely on the sidewalk. In our system, an assistant with normal vision is asked to create the database for the places where the blind user usually visits. At each sampling spot of these places, the assistant takes a few photos that cover different viewing directions around the sampling spot to create a panorama image. After the installation of the database, the blind user is equipped a camera while he or she is walking around these places. For each captured image by the camera, the proposed system finds the most similar panoramic part in the database to identify the location and the orientation of blind user. With an image-to-image matching to warp the labels from the matched panoramic part to the captured image, our system can roughly infer the labeling of the contents within the captured image. Finally, based on the inferred labels, our system can identify situations that could be dangerous to the blinds.

## 誌謝

首先非常感謝我的指導教授 王聖智老師，在念研究所的期間，老師的潛移默化之下，習得諸多理工知識，尤其是從老師身上學習到了很多報告的技巧，以及做研究正確的方法與邏輯。謝謝老師仔細的指導，讓我在這兩年如沐春風！再來感謝敬群學長、慈澄學長、禎宇學長、維辰學長、家豪學長以及其他眾多實驗室學長們提供的寶貴意見，讓我的研究更為完善。也謝謝實驗室的好夥伴：玉書、韋弘、開暘、郁霖，以及學弟妹們。與你們相處的日子非常開心，實驗室總是充滿笑聲，讓我覺得一點也不孤獨！最後感謝我的父母，有你們不求回報的支持和鼓勵，我才能好好的完成課業及研究。



# Content

Chapter 1.	Introduction.....	1
Chapter 2.	Backgrounds .....	3
2.1.	Ultrasonic, Laser and RFID Travel Aid Systems.....	4
2.1.1.	Ultrasonic Sensors .....	5
2.1.2.	Laser Sensors .....	6
2.1.3.	RFID .....	7
2.2.	Vision-based Travel Aid Systems .....	8
2.2.1.	Landmark Targeting .....	9
2.2.2.	Scene Understanding .....	11
2.2.3.	Vision-based Guiding Systems .....	13
Chapter 3.	Proposed System.....	16
3.1.	Sub-Database Retrieval.....	18
3.1.1.	Building Panoramic Database.....	19
3.1.2.	Sub-Database Retrieval for Neighboring Scenes.....	20
3.2.	Determination of Facing Direction .....	21
3.2.1.	Global Feature: Gist.....	22
3.2.2.	Spatio-temporal Constraint for Search Window .....	25
3.3.	Scene Alignment and Label Transformation.....	27
3.3.1.	SIFT Flow .....	28
3.3.2.	Panoramic Approach.....	32
3.4.	Dangerous Situation Detection .....	33
3.5.	Temporal Interpolation.....	37
3.5.1.	Motion Prediction .....	38
3.5.2.	Label Propagation .....	38
Chapter 4.	Experimental Results .....	40
4.1.	Label Results of Different Approaches .....	40
4.2.	Outdoor Experimental Results within NCTU.....	42
4.2.1.	Database Setup.....	42
4.2.2.	Experimental Results in Test Environments .....	43
4.2.2.1.	Results of Database Retrieval .....	44
4.2.2.2.	Cloudy Day .....	45
4.2.2.3.	Sunny Day and Evening Time .....	48
4.2.2.4.	Experimental Data .....	49
Chapter 5.	Conclusions.....	53
References.....		54

# List of Figures

Figure 1-1 Some examples of dangerous situation while walking on a sidewalk. Our goal is to identify dangerous situations based on the captured images. ....	2
Figure 2-1 Prototype of Navbelt [2].....	5
Figure 2-2 Functional components of Guide cane [3] .....	6
Figure 2-3 The layout of the hand-held equipment of virtual white cane.....	7
Figure 2-4 The framework of the navigation system in [7] using RFID .....	8
Figure 2-5 Block diagrams of the framework in [8] .....	10
Figure 2-6 Some results of path detection in [8].....	11
Figure 2-7 Example results from Textonboost [10] for image understanding .....	12
Figure 2-8 Example result of SuperParsing in [11] .....	13
Figure 2-9 System overview of [12] .....	14
Figure 2-10 Multi-level surface patch models for [12].....	14
Figure 2-11 Guiding result of [13] .....	15
Figure 3-1 Block diagram of proposed system .....	17
Figure 3-2 Major challenges: (a) variations of scene appearance, (b) feature similarity between road and sidewalk, and (c) very different scene contents from different viewing directions.....	18
Figure 3-3 Stitching 16 images of different viewing directions to form a panoramic image.....	19
Figure 3-4 An example of three adjacent sub-databases. Here, all the panoramic images have the same arrangement of directions. ....	20
Figure 3-5 Labels of a panoramic image .....	20
Figure 3-6 Garmin’s USB-version GPS 18.....	21
Figure 3-7 Different scene categories .....	22
Figure 3-8 Gabor filter banks for multiple scales and orientations .....	23
Figure 3-9 Filter bank responses.....	24
Figure 3-10 Block diagram of Gist feature extraction .....	24
Figure 3-11 Visualization of Gist feature for different image views .....	25
Figure 3-12 Slow motion of blind user reduces searching area for the panoramic images .....	26
Figure 3-13 (a) Input frame. (b) The best matched image portion. ....	27
Figure 3-14 Visualization of SIFT features .....	29
Figure 3-15 (a) Input frame. (b) Best match from database. (c) Warped image.....	30
Figure 3-16 (a) Best match and the corresponding labels. (b) Input frame and the inferred labels.....	30
Figure 3-17 Different size of search window for optical flow and SIFT flow .....	31

Figure 3-18 Illustration of poor alignment. (a) Input frame. (b) Best match. (c) Warped image. ....	31
Figure 3-19 Panoramic extension of original support image.....	32
Figure 3-20 More information is acquired by using panoramic approach. Top: extended support image. Bottom: input frame. Color lines indicate feature correspondence .....	33
Figure 3-21 Region of interest that models human’s visual attention area.....	33
Figure 3-22 Decision rules for direction turning .....	36
Figure 3-23 Flow diagram of dangerous situation detection .....	36
Figure 3-24 Simplified architecture by using temporal information .....	37
Figure 3-25 Camera panning caused by the turning of the user .....	38
Figure 3-26 Histogram of SIFT flow magnitudes in the horizontal direction when the user turns left. The green words indicate the inferred camera status.....	39
Figure 3-27 Histogram of SIFT flow magnitudes in the horizontal direction when the user walks straight. The green words indicate the inferred camera status. ....	39
Figure 4-1 (a) Single-view support image, (b) panoramic-view support image, (c) warped result from single-view image, (d) warped result from panoramic-view image, (e) ground truth labels, (f) mapped labels based on single-view support, and (g) mapped labels based on panoramic view. ....	41
Figure 4-2 (a) Single-view support image, (b) panoramic-view support image, (c) warped result from single-view image, (d) warped result from panoramic-view image, (e) ground truth labels, (f) mapped labels based on single-view support, and (g) mapped labels based on panoramic view. ....	41
Figure 4-3 Our test routes in NCTU .....	42
Figure 4-4 Scene appearances.....	42
Figure 4-5 Results of database retrieval for walking forward with some pedestrians passing by. (a) Frame index, (b) input frames, and (c) the best match from the panoramic sub-database. ....	44
Figure 4-6 Results of database retrieval for a panning case. (a) Frame index, (b) input frames, and (c) the best match from the panoramic sub-database. ....	44
Figure 4-7 The case of walking forward in safe situation. (a) Frame index. (b) Input frames. (c) Inferred labels. (d) Outcome of dangerous situation detection. ....	45
Figure 4-8 The case of turning to a wrong direction. (a)Frame index. (b) Input frame. (c) Inferred labels. (d) Outcomes of dangerous situation detection. (e) Suggested turning direction. ....	46
Figure 4-9 The case of approaching to the border of sidewalk and road. (a) Frame	



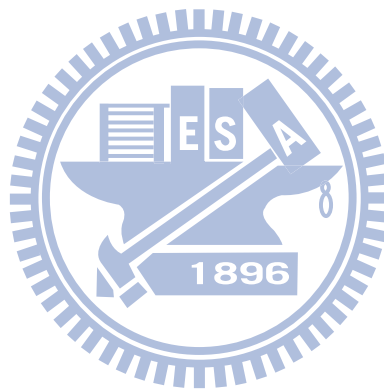
index. (b) Input frames (c) Inferred labels. (d) Outcome of dangerous situation detection. (e) Suggested turning direction. ....47

Figure 4-10 The case of little sidewalk area in front of the user. (a) Frame index. (b) Input frame. (c) Inferred labels. (d) Outcome of dangerous situation detection. (e) Suggested turning direction. ....47

Figure 4-11 Test results in sunny day. (a) Input frames. (b) Inferred label. (c) Outcome of dangerous situation detection. (d) Suggested turning direction. ....48

Figure 4-12 Some examples at evening time. (a) Input frame. (b) Inferred labels. (c) Outcome of dangerous situation detection. (d) Suggested turning direction. ....49

Figure 4-13 Ground truth definition (a) to (c): apparent cases, (d) to (f): use the location of border to determine whether it is a dangerous situation. ....50



# List of Tables

Table 4-1 Accuracy of sub-database retrieval.....	49
Table 4-2 Definition of false positive and false negative .....	50
Table 4-3 Experimental data at cloudy day and comparison of single-view approach	51
Table 4-4 Experimental data under different lighting conditions .....	51
Table 4-5 Computational speed for our system .....	52



# Chapter 1.

## INTRODUCTION

For people with normal vision, taking different activities outdoors, like shopping or playing sports, is just a piece of cake. However for thousands of blind people, even walking on sidewalk safely is not a simple task. Because visually impaired people cannot see the world clearly, they may be unconscious of walking into a wrong way. In order to take a safe travel outdoors, visually impaired people usually need a white cane or a guide dog to assist them. But the tactile information passed from the end of white cane is not always robust, and a guide dog may get easily interfered by the environment. With the rapid development of vision-based technologies, one may think if there is some kind of “virtual eyes” for blind people. That is, whether we can utilize algorithms of computer vision to provide a more convenient life for blind people?

With the booming information technology in recent years, many portable devices can surf over internets and connect to global positioning system (GPS). Besides, the computational speed for portable devices is much faster than before. On the other hand, researchers have found that blind people tend to travel around places that are familiar to them. With the above two phenomena, we may be able to develop some kind of guiding system for blind people. For example, for a given environment, we can create a database beforehand. After that, when a blind user walks into this environment, he/she can use a portable device equipped with GPS to identify his/her location and to extract the corresponding information from the database to assist his/her movement within the scene.

In this thesis, our system is built based on the aforementioned data-driven framework. Given a video, our system automatically labels the safe walking area and determines whether the current situation is dangerous or not for the blind people. Some examples of dangerous situations are shown in Figure 1-1. Here we combine database retrieval and image-to-image dense matching to label the walking areas in a local environment. Based on the information extracted before, the system helps blind people to identify dangerous situations while walking. The red areas in Figure 1-1 represent the road regions and the green areas indicate the sidewalk regions.

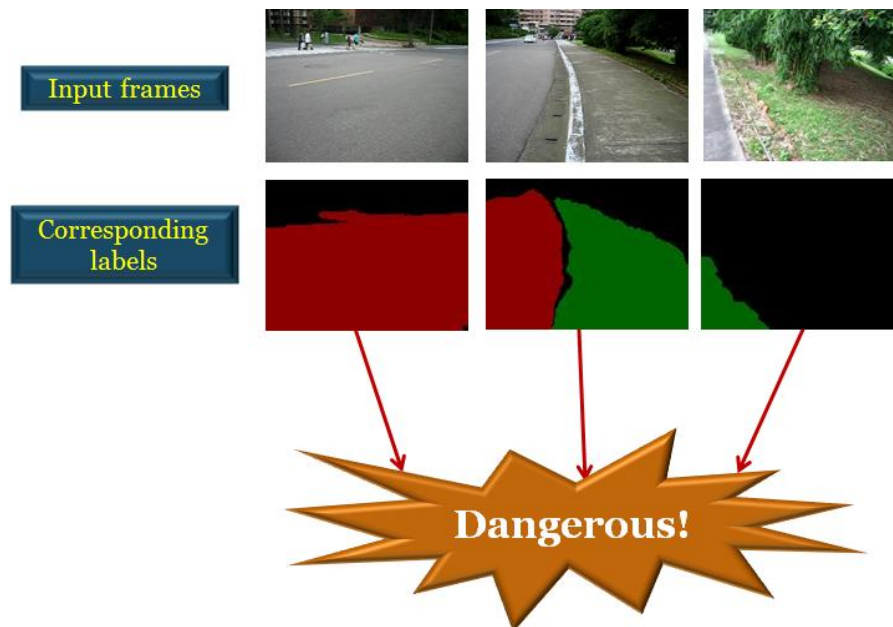


*Figure 1-1 Some examples of dangerous situations while walking on a sidewalk.  
Our goal is to identify dangerous situations based on the captured images.*

In the following chapters, we will first introduce a few kinds of electronic aid systems for blind people in Chapter 2. In Chapter 3, we present the proposed system for safe area labeling and dangerous situation detection. Some experimental results will be shown in Chapter 4. Finally, we will give our conclusion in Chapter 5.

# Chapter 2.

## BACKGROUNDS

Because visually impaired people cannot see the world clearly, they need something to help them walk safely indoors and outdoors. Generally speaking, white canes and guide dogs are the most popular travel aids for blind people. White cane is a hand-held facility that can assist blind people to notice some drop-offs on the walking area or some obstacles in front of him/her. On the other hand, guide dogs help blind users to find the safe walking direction. For over thirty years, many technologies have been applied to develop supporting devices that assist visually impaired people to live in a more convenient way. According to [1], these technologies are classified into three categories based on their functionalities. These three categories are listed as follows.

1) Electronic travel aids (ETAs):

ETA systems help blind people to roughly know the environment. For instance, some systems can tell whether there is an obstacle in front of the user or not. Some other systems can tell when crucial objects appear near the user.

2) Electronic orientation aids (EOAs):

Because of the poor vision of blind people, they may lose the sense of direction while walking. Hence, some systems are developed to tell blind people which direction they are facing to.

3) Position locator devices (PLDs):

Global Positioning System (GPS) is the most popular PLD. GPS feature has been

integrated in many 3C devices, like smart phones. Blind people can easily know their current location if they bring a GPS device with them.

EOA and PLD systems have been developed and widely used in the last decades. On the other hand, ETA systems have been developed over the past thirty years. In this thesis, we focus on the usage of ETA devices. In Section 2.1, we will introduce some electronics travel aid systems using ultrasonic, laser, and RFID technology. In Section 2.2, we will introduce systems using vision sensors, and introduce what kinds of functionalities can be achieved by computer vision based algorithms.

## **2.1. ULTRASONIC, LASER AND RFID TRAVEL AID SYSTEMS**

As the name suggests, sensor-based systems are set up by using some specific sensors, like ultrasonic sensors or laser sensors. Since 1960's, many evolving technologies have been proposed for the navigation aids of blind people. Ultrasonic and laser sensors are usually used to detect obstacles in front of blind people, while RFID systems can help blind people to obtain some information about the local environment.

In Section 2.1.1 we will introduce two guidance systems that use ultrasonic sensors. In Section 2.1.2, we will introduce some approaches that use lasers. In Section 2.1.3, we will introduce the RFID framework for the assistance of visually impaired people.

## 2.1.1. Ultrasonic Sensors

In the 1990s, many researchers discovered that obstacle avoidance systems for mobile robots were highly related to the guiding system for blind people. The Navbelt [2] was a typical example. The technology used in Navbelt is originally developed for mobile robot guidance. The designers claim that Navbelt enables the user to avoid obstacle safely while walking in unknown environments. Moreover, this system was implemented to be portable and its prototype is shown in Figure 2-1.



*Figure 2-1 Prototype of Navbelt [2]*

The Navbelt is equipped with eight ultrasonic range sensors, a portable computer, and earphones. These ultrasonic sensors are used to detect obstacles. The computer converts the received signals to an information map that records the orientations and distances to the obstacles in front of the blind user. Navbelt has two modes, image mode and guidance mode. In the image mode, the system tells a user the orientations and distances to the obstacles by using different tones and amplitudes via earphones. On the other hand, in the guidance mode; it assumes that the momentary direction and destination of user are known. Hence, the Navbelt can use the sensors signal to guide the user. However, in reality, the blind man would need an assistant with normal

vision to help him/her to walk for a while so the system could know the desired direction for the blind.

By the same research group, Guide cane [3] is developed as an updated version of Navbelt. This system can be held as a white cane, as shown in Figure 2-2. By detecting obstacles, it guides the user to walk along the safer way. It would be convenient to use this system and the user won't need too much training time to get used to the system.

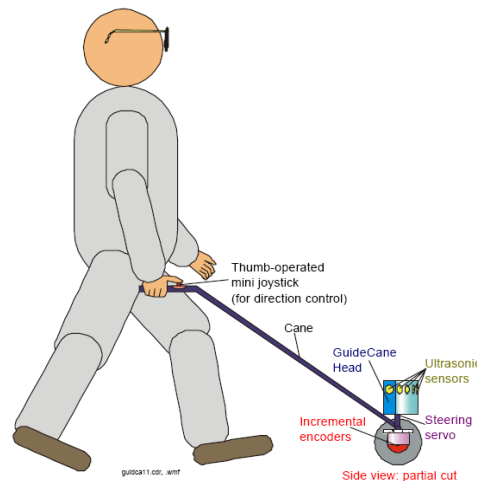


Figure 2-2 Functional components of Guide cane [3]

## 2.1.2. Laser Sensors

When setting up a travel aid device for blind, laser sensors are another choice. Like the laser cane in [4], laser sensors are also used for obstacle avoidance. In the work of [5, 6], the authors developed a hand-held environment discovering equipment named “virtual white cane”. In their system, they use a laser-based range sensor and a CCD camera. The system layout is illustrated in Figure 2-3. When a laser beam is emitted from a laser pointer, the reflection is to be detected by the well aligned CCD sensor array. When the blind user swings the hand-held equipment around, the local



environment information will be captured. Based on the time profile produced by the light, the equipment can analyze the data to estimate some environmental features, such as steps and drop-offs. However, for an outdoor environment, the laser may be jammed by a lot of unexpected noise.

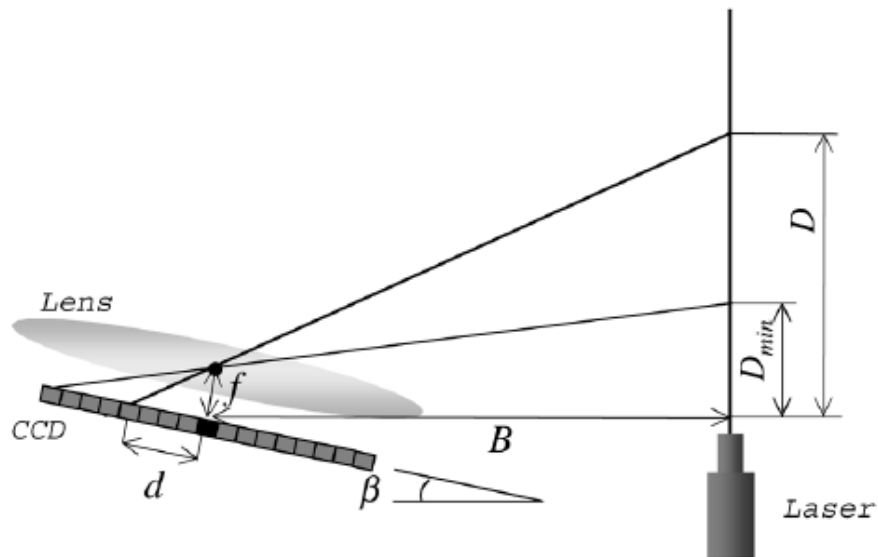
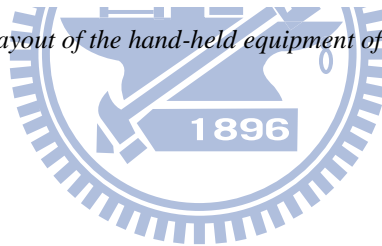


Figure 2-3 The layout of the hand-held equipment of virtual white cane



### 2.1.3. RFID

For outdoor walking, visually impaired people are used to find blind tiles in order to follow them by hand-held white cane. In [7], they built a large-scale guiding framework based on Radio Frequency Identification (RFID) devices and wireless communication technology. In their framework, RFID tags, which can offer useful information provided from the centralized information system, are buried under the roads. With an RFID reader embedded in the blind cane, the blind users can get some helpful information like the status of traffic light or the location of the nearest bus station. An illustration of this framework is shown in Figure 2-4. Even though this framework provides sufficient assistance for visually impaired users, it would require

a lot of efforts to create such a large-scale comfortable environment.

For obstacles detection, sonar- and laser-based travel aids have boomed for many years. A major advantage of these devices is their efficient computation. However, these devices can only detect objects that have an apparent 3-D shape. For example, the signals emitted by sonar sensors are not able to detect sidewalks, curbs, or roads. Another drawback is their high cost.

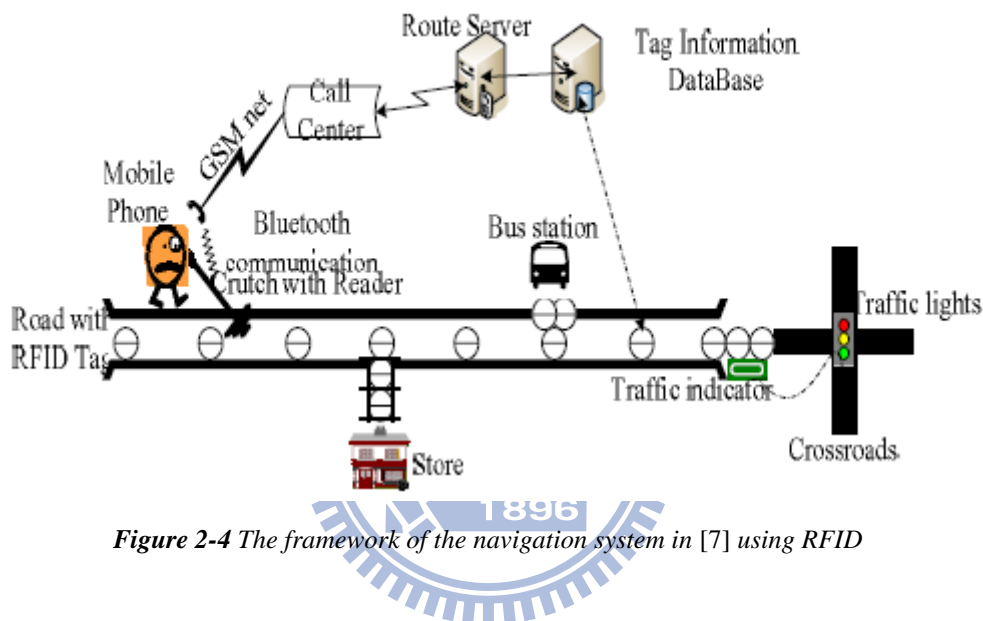


Figure 2-4 The framework of the navigation system in [7] using RFID

## 2.2. VISION-BASED TRAVEL AID SYSTEMS

As mentioned before, electronics travel aids (ETAs), which make use of ultrasonic and laser sensors, have been developed to help blind user's daily activities in both indoor and outdoor environments. Compared to these popular technologies, vision-based approaches can provide some other advantages. For example, image sensors, like webcams, have low cost and low power demands. In theory, one can use cameras to capture all the visual information in front of the blind user. In other words, camera can be seen as "virtual eyes" for the blind people. With this property, we can

develop much more fantastic functionality to help the blinds by using computer vision based algorithms.

In computer vision, object detection and recognition are crucial and challenging. Given an image, there may be some informative objects for traveling, like waymarks, crosswalks, traffic lights, and sidewalks. In recent years, some researchers have investigated the issues of automatic detection, recognition, and segmentation of multiple objects in an image. Besides, the scene understanding issue has been raised to decompose the given image into several semantically meaningful regions. If the scene understanding algorithms can roughly identify the spatial layout of the scene, this useful message can be passed to visually impaired users to help them understand their current environments.

In Section 2.2.1, we will introduce a system for landmark targeting. The system detects the prominent objects which are specific and important for blinds. In Section 2.2.2, we will introduce a few state-of-the-art scene understanding algorithms. These works may achieve multi-class object segmentation and labeling. In Section 2.2.3, we will introduce some vision-based guidance systems.

## **2.2.1. Landmark Targeting**

While taking a walk outdoors, we usually follow sidewalks for the concern of safety. On the other hand, we also need to pay attention to some obstacles such as cars and people to avoid collision. In [8], the authors proposed a cheap and wearable facility for visually impaired people. The block diagram of the overall system is illustrated in Figure 2-5.

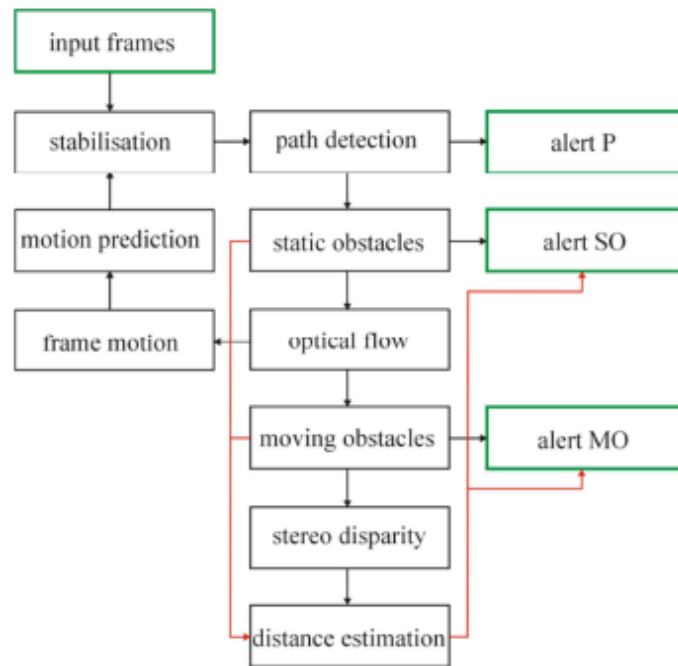


*Figure 2-5 Block diagrams of the framework in [8]*

In their system, they first search the paths in the input frame. The path detection window is initially set to be under a horizontal line that is close to the middle of the frame. After the initial frame, the position of the horizontal line is updated dynamically based on the detected path borders and the corresponding vanish points of previous frames. After that, the Canny edge detector is used to generate an edge map. In their approach, the authors assume the shape of the path in front of the user is simple. Hence, the gradient orientations of the sidewalk borders are restricted to a certain range. Besides, they assume the borders would intersect at a vanish point. Based on the above assumptions, Hough transform is used to search for lines within the path detection window. Some path detection results are shown as Figure 2-6. After path detection, edge and texture cues are utilized to detect static obstacles. Moreover, the optical flow method is used to capture moving obstacles such as human walking on the sidewalk. Finally, the stereo disparity can provide the distance information of the detected obstacles. Since the edge and texture cues can easily get interfered by occlusion or shades, their work is currently limited to simple scenes only.

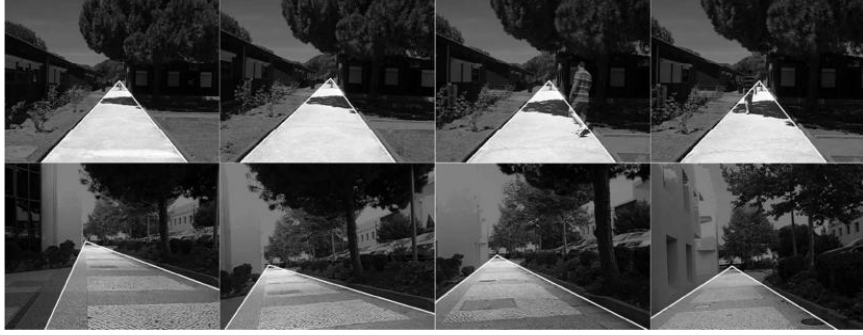


*Figure 2-6 Some results of path detection in [8]*

## 2.2.2. Scene Understanding

In current multi-class object recognition/segmentation algorithms, Markov random field (MRF) or conditional random field (CRF) [9] is usually adopted to incorporate different features in a single model. In [10], they proposed an approach to learn a discriminative model of object classes which combines texture, layout, and context information efficiently. They also use conditional random field to learn and combine texture-layout, color, location, and edge cues in a unified model, as expressed in Eq. 2-1. Here, the notation  $\mathbf{c}$  indicates the class label and  $\mathbf{x}$  indicates the image.

$$\begin{aligned} \log P(\mathbf{c} | \mathbf{x}, \theta) = & \sum_i (\psi_i(c_i, \mathbf{x}; \theta_\psi) + \pi(c_i, x_i; \theta_\pi) + \lambda(c_i, i; \theta_\lambda)) \\ & + \sum_{(i,j) \in \mathcal{E}} \phi(c_i, c_j, \mathbf{g}_{ij}(\mathbf{x}); \theta_\phi) - \log Z(\theta, \mathbf{x}) \end{aligned} \quad \text{Eq. 2-1}$$

In this equation, the first term is texture-layout potentials; the second term is color potentials; the third term represents location potentials; the fourth term is edge potentials that measure the class located in the two sides of the edge; and  $Z$  is the partition function term to normalize the distribution. In the training stage, they want to learn the weighting  $\theta$  for each feature term. In the label inference stage, they apply the learned model to the image and try to associate object category label with pixels or

other image representations (see Figure 2-7). Finally, the input image is partitioned to semantic meaningful regions. However, there may be some drawbacks in these learning-based methods. One is that it is hard to adjust the number of object categories after the model is determined. Moreover, if the features of different object classes are similar, the inference results may be wrong.

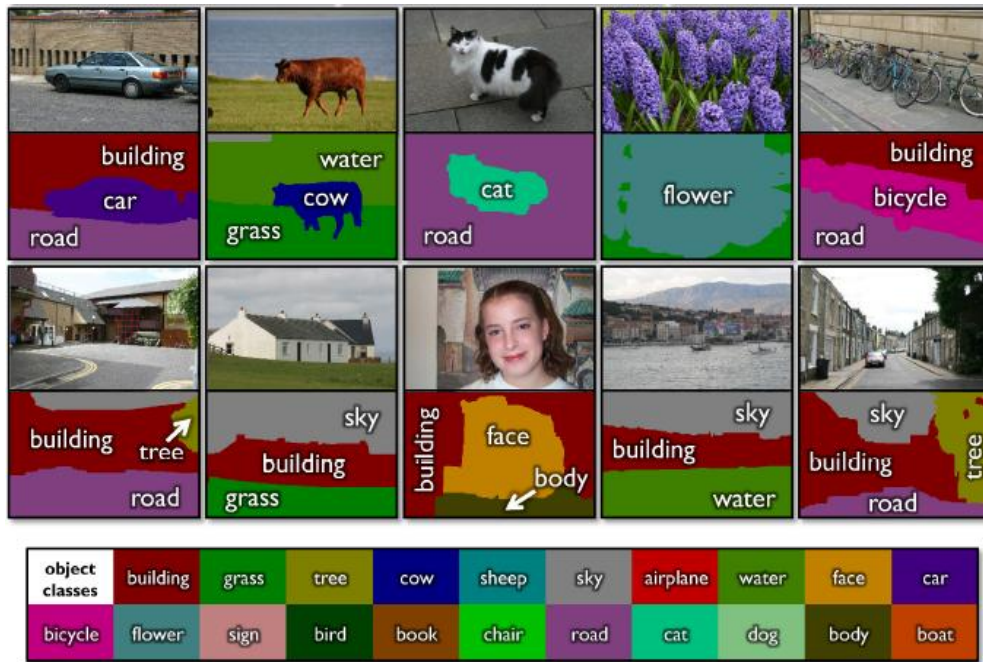


Figure 2-7 Example results from Textonboost [10] for image understanding

On the other hand, the authors in [11] adopted a data-driven approach. They first retrieve similar scene type from the retrieval set and generate super-pixels for the query image by using bottom-up segmentation. The super-pixels are described by shape, location, texture, and appearance features. After those two steps, the likelihood ratio score of object classes for each super-pixel can be obtained. They encode contextual constraints with the help of Markov random field, as expressed in Equation 2-2. Here,  $c$  also denotes the class label and  $s_i$  represents the  $i^{\text{th}}$  super-pixel. For each semantic class is associated with a geometry class, such as ground, sky, or vertical. Finally they jointly determine the geometric labels and semantic labels by optimizing the objective function in Equation 2-3, which is an extension of Equation 2-2. Here,

the notation  $\mathbf{g}$  represents geometric class label. The last term of Equation 2-3 enforces the coherence between geometric class and semantic class. This term is zero when these two labels are matched correctly, and is one otherwise. An example is shown in Figure 2-8.

$$J(\mathbf{c}) = \sum_{s_i \in SP} E_{data}(s_i, c_i) + \lambda \sum_{(s_i, s_j) \in A} E_{smooth}(c_i, c_j) \quad \text{Eq. 2-2}$$

$$H(\mathbf{c}, \mathbf{g}) = J(\mathbf{c}) + J(\mathbf{g}) + \mu \sum_{s_i \in SP} \varphi(c_i, g_i) \quad \text{Eq. 2-3}$$

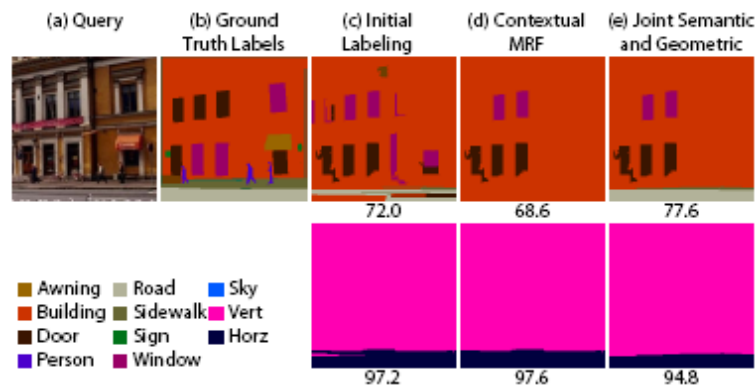


Figure 2-8 Example result of SuperParsing in [11]

### 2.2.3. Vision-based Guiding Systems

In [12], the authors proposed a wearable and stereo-vision based navigation system for blind people. A pair of cameras is used as the data acquisition device. They also combine visual odometry and Simultaneous Localization and Mapping (SLAM) algorithm into their work. By utilizing camera pose estimation with dense 3D information from stereo-vision, a vicinity map is created for the surrounding environment. The block diagram of their system is illustrated in Figure 2-9.



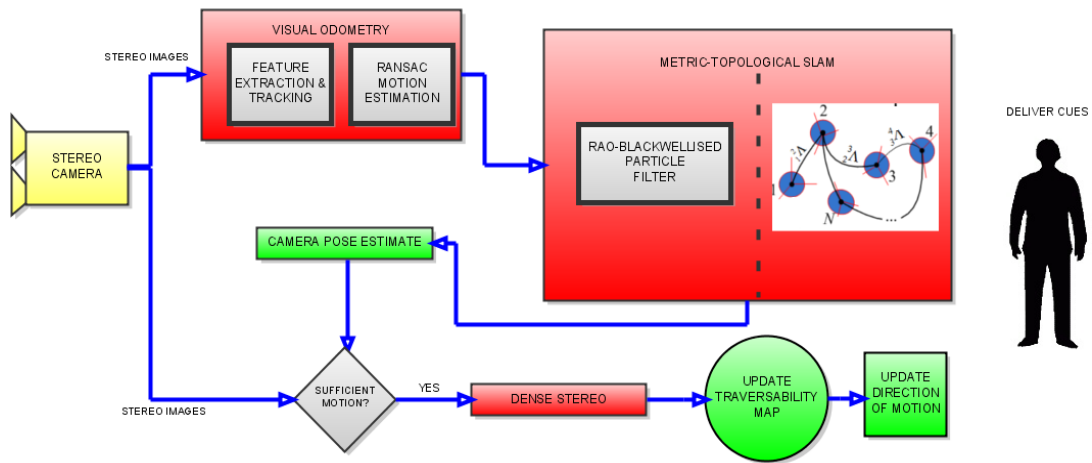


Figure 2-9 System overview of [12]

However, the main limitation of their work comes from the stereo-vision architecture. When the local environment is low-textured, the depth map produced by the stereo camera system will not be accurate enough. Some surface model results are shown in Figure 2-10, where red regions represent vertical surfaces, green regions represent horizontal surfaces, and the red cones represent camera orientations.

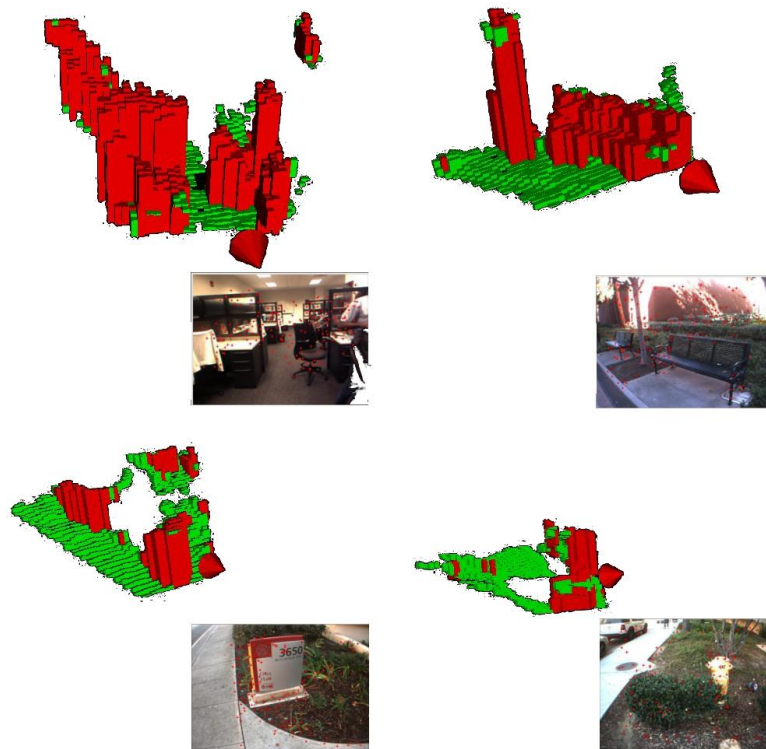
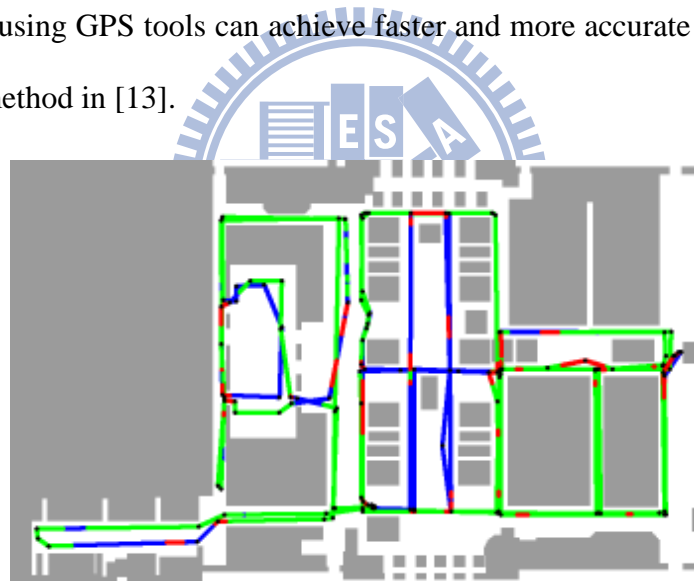


Figure 2-10 Multi-level surface patch models for [12]



In [13], the authors proposed a data-driven framework. In their system, training video sequences were taken beforehand. They select some key frames as reference data and perform registration with respect to 2D positions and orientations. For every key frame, they extract Speeded Up Robust feature (SURF) [14] and GIST feature [15]. When the query image is captured, the user will know where he/she is by matching feature to the reference images in the database. The scene continuity is modeled by the hidden Markov model (HMM). The guiding result is shown in Figure 2-11, where black dots represent key frame locations, blue lines represent ground truth location of query frames, green lines represent covered ground truth, and red parts represent the locations where error is over ten meters from the ground truth. For outdoor cases, using GPS tools can achieve faster and more accurate localization than the proposed method in [13].



*Figure 2-11 Guiding result of [13]*

# Chapter 3.

## PROPOSED SYSTEM

While traveling outdoors, walking on the sidewalk is the commonest action. For people who have normal vision, it's easy to change momentarily the walking direction to avoid dangers. However, for thousands of blind people, they are afraid of walking in a wrong direction, which may cause fatal dangers to them. Hence, automatically detecting the walking area in front of blind people could be very helpful to them. For blind people, the white cane is a commonly used tool. However, white canes cannot provide reliable tactile information to help blind users distinguish curb from sidewalk. On the other hand, the state-of-the-art sonar- and laser-based systems cannot detect the unobvious drop-offs on the sidewalk borders in outdoor environments either. To achieve this kind of assistance, we aim to utilize computer vision algorithms.

Up to now, some nowadays popular scene understanding algorithms learn a model to classify different image regions into corresponding object categories. However, due to the multiple outdoor scene appearances and the view-dependent variations of scene structure, a single model may not be able to efficiently handle the scene understanding problem. Moreover, the scene understanding algorithms may get poor inference results when the features of different objects appear to be similar.

From the habit investigation of blind people, we learn that blind people are used to walk around in an environment that they are familiar with. This phenomenon inspires us to adopt a data-driven approach. On the other hand, many modern portable devices are able to surf over the internet and to receive GPS signals to identify their geographic locations. Hence, we can set up a database for the places where the blind

user tends to visit. When the blind user walks around these places, he or she can use the information captured by his/her portable device and the identified geographic location to retrieve appropriate reference data from the already installed database in order to achieve safer navigation.

In this thesis, the goal of our system is to label the walking area for the current scene in front of the blind user. First, the blind user will use some geographic locating device like GPS to identify his/her current location. Based on the current location, the system retrieves a few panorama images from the database to represent the neighboring scenes of the blind user. After that, with respect to the image captured by the portable camera hung in front of the blind user, the system adopts a fast global feature matching method to search within the panoramas the most similar scene. In practice, the captured image and the matched image data would be roughly the same. Since we have already labeled some important objects, like roads and sidewalks, in the panorama images, we can warp the labels of the matched image to form the labels of the captured image. With the mapped labels, the system can roughly understand the current scene in front of the user and detect some situations that could be dangerous to the user. Figure 3-1 shows the block diagram of our framework.

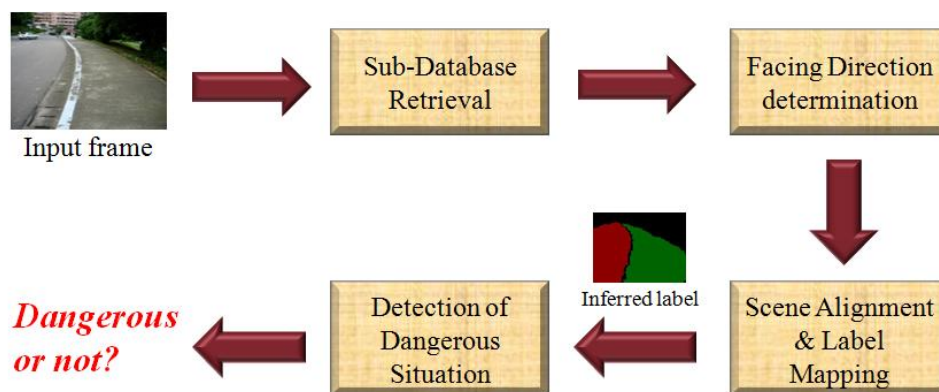


*Figure 3-1 Block diagram of the proposed system*

The challenges of our system includes: (1) the scene appearance may vary a lot in an outdoor environment; (2) the features of road and sidewalk may be similar to each other; and (3) the observed scene may vary a lot with respect to different viewing directions. Some examples of these challenges are shown in Figure 3-2. To solve the first and second challenges, we adopt a database retrieval approach to search for the most similar image that interprets the surrounding scene. To solve the third challenge, the database is composed of panoramic images. In Section 3.1, we will explain the detail of database construction and sub-database retrieval. In Section 3.2, we will introduce the algorithm that determines the facing direction of the user. In Section 3.3, we will introduce the processes of scene alignment and label mapping. In Section 3.4, we will introduce the detection of dangerous situations. In Section 3.5, we will tell how to use the temporal information to simplify our system.

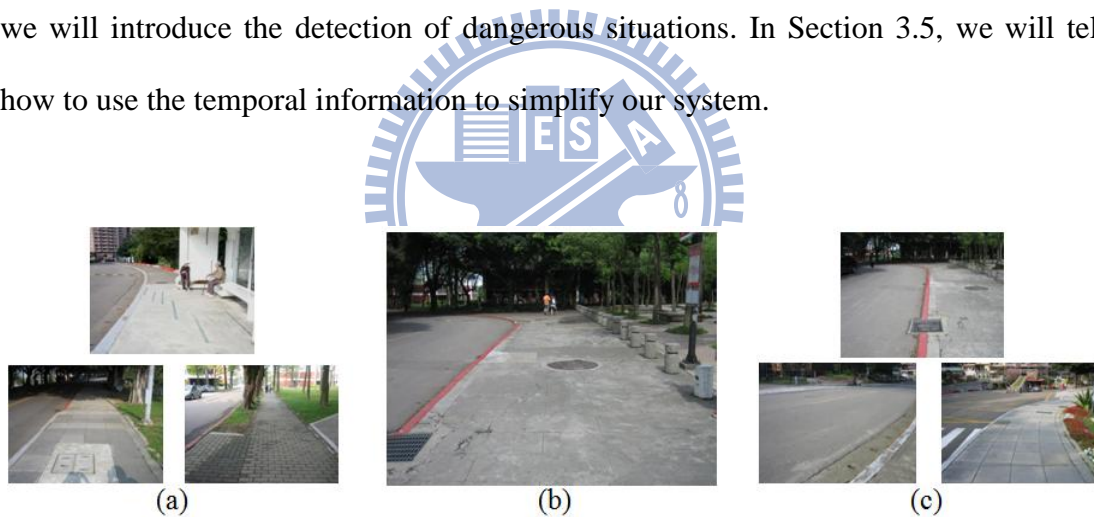


*Figure 3-2 Major challenges: (a) variations of scene appearance, (b) feature similarity between road and sidewalk, and (c) very different scene contents from different viewing directions.*

## 3.1. SUB-DATABASE RETRIEVAL

In this section, we will introduce how to build the database and how to retrieve the sub-database that contains the panoramic images of the neighboring scenes.

### 3.1.1. Building Panoramic Database

In order to safely walk around in the campus of National Chiao Tung University, we should set up a database that represent the scenes around a few sampling spots in the campus. In the following paragraphs, we will explain how we install the database. At each sampling spot, we took photos at 16 different viewing directions to model the possible views that a person with normal vision may see. These 16 photos were stitched together to form a 360-degree panoramic image, as shown in Figure 3-3. When we took the photos, our camera is held at about 1.6 meters height. Moreover, we took these photographs in cloudy days in order to reduce the strong-light effect and the strong shade interference.

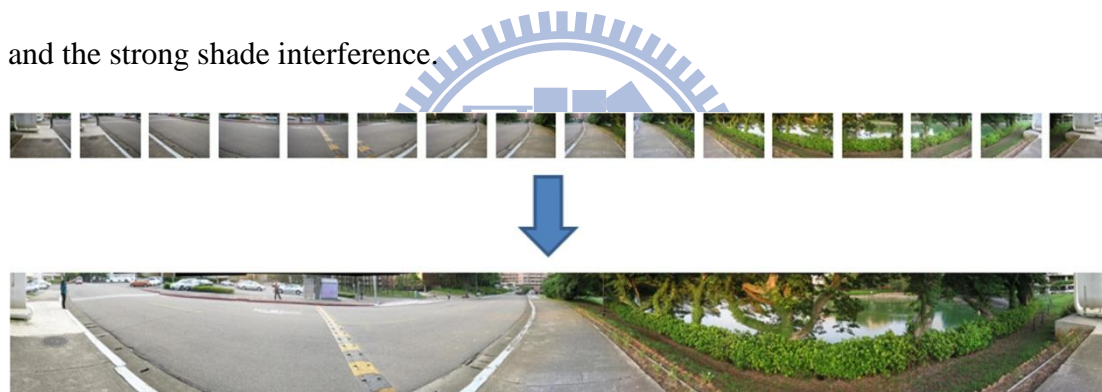


*Figure 3-3* Stitching 16 images of different viewing directions to form a panoramic image

To stitch these photos of different viewing directions, we use the Hugin panorama creator, which allows several overlapping photographs taken at the same place to be merged into a large photo. This panorama creator matches the Scale Invariant Transform (SIFT) features of the overlapping regions of two images to align and transform photos to create a panoramic image. Before stitching images, we have to choose an anchor image at a certain direction to achieve the same arrangement of the panorama while stitching, as shown in Figure 3-4. The white balance and exposure are also corrected for each image based on the anchor image.



*Figure 3-4 An example of three adjacent sub-databases. Here, all the panoramic images have the same arrangement of directions.*

After having obtained the panoramic images, we label each panorama to create the annotations. Here, we use the on-line labeling tool LabelMe [16] to label the important regions such as sidewalks and roads in the panorama, as shown in Figure 3-5. Inside the green polygons are labeled as sidewalk regions, while inside the pink polygons are labeled as road regions.



*Figure 3-5 Labels in a panoramic image*

### **3.1.2. Sub-Database Retrieval for Neighboring Scenes**

To interpret the surrounding environment for the user, we don't need to search over the whole database but only need to check a local sub-database. Intuitively, there may be some degree of scene discontinuities between adjacent sub-databases. Hence, we may not be able to get good interpretation of the surrounding environment if we only check the nearest panoramic image. Moreover, the routes in campus are not always straight. Hence, the scene at some sampling spots may have complex spatial layout. To deal with these problems, we search the panoramic images at three nearby sampling spots.

Our system is a kind of wearable aid system for visually impaired user. In real implementation, we use a GPS device to find user's location. Here we use the Garmin

GPS 18 portable device, as shown in Figure 3-6. Garmin GPS 18 updates the location for every second and has a USB connection that can be easily connected to wearable equipment. When this device is connected to a notebook, we use the open source software Franson GpsGate 2.6 to extract NMEA data from the device to get the current latitude. Like in [17], we have tagged all of our panoramic images with the corresponding GPS coordinates. Hence, by using the Garmin GPS 18 to get the current GPS location, we can identify the three panoramic images that have the shortest geographic distance with respect to the current location. These three panoramic images are treated as the sub-database for subsequent processes.



*Figure 3-6 Garmin's USB-version GPS 18*

## **3.2. DETERMINATION OF FACING**

### **DIRECTION**

After finding the sub-database of three panoramic images at nearby sampling spots, as shown in Figure 3-4, we search within each panoramic image to find the image portion that is most similar to the current front-view image of the user. This action can be seen as modeling the “virtual sight” for visually impaired people. With the matched image portion, the blind user will be able to roughly know the current



direction he/she is facing to.

In this step, we want find the most similar part efficiently via feature matching. Many popular image matching algorithms in the literature, such as SIFT or Speeded Up Robust Feature (SURF), are developed to match local regions. With these approaches, the matching result may get easily interfered by unexpected objects in the scene, like walking people or cars. In our approach, we describe the whole image in terms of a single global feature vector, by which we can achieve lower computational complexity and lower noise interference.

In the literature, global features are usually used to solve scene categorization problems. Different scene categories usually have different appearances, as shown in Figure 3-6. For example, street scenes may contain lots of vertical and horizontal lines, while natural scenes usually contain undulating contours. In our case, we want to utilize a global feature to search for the matched image portion in the panoramic images. For every panoramic image in the sub-database, we partition it into 32 overlapping sub-images along the horizontal direction. Hence, given the image captured by the camera, we try to find the best match among the 32 (sub-images per panorama)  $\times$  3 (panoramas per sub-database) = 96 sub-images. In Section 3.2.1, we will introduce the widely used global feature “gist”. In Section 3.2.2, we will introduce how to model the blind’s slow motion in the global matching process.



*Figure 3-7 Different scene categories*

### **3.2.1. Global Feature: Gist**

Gist [18] is a low dimensional global feature, which encodes different responses



to human eyes from different spatial regions of an image. In other words, the gist feature models coarsely the edge and texture information of different spatial regions in an image. This feature has been tested for various kinds of applications, like scene categorization and image retrieval, and has demonstrated reliable performance. Moreover, with the low dimension of this feature, we can efficiently measure the similarity between two images.

The gist descriptor performs Fourier transform analysis after the pre-processing that reduces boundary artifacts and normalizes the local contrast. To construct the gist feature, the image is convolved with a multi-scale oriented Gabor filter bank, as shown in Figure 3-8. The Gabor filter bank is composed of four scales, with each scale having eight orientations. The filter bank responses are shown in Figure 3-9.



**Figure 3-8** Gabor filter banks for multiple scales and orientations

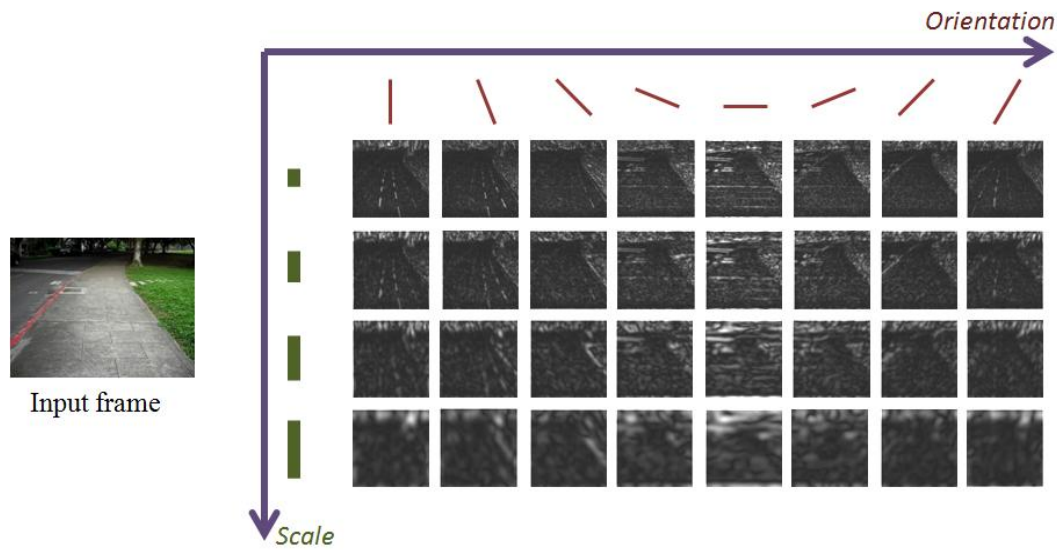


**Figure 3-9** Filter bank responses

Next, for each filter output, we average the magnitude response within each  $4 \times 4$  non-overlapping blocks of the image. These responses are stacked together to form a  $4 \times 4 \times 4 \times 8 = 512$  dimensional feature vector. The overall flow chart of the gist feature extraction is shown in Figure 3-9.

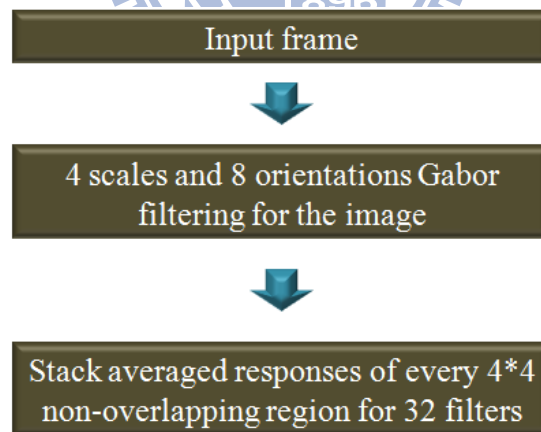


**Figure 3-10** Block diagram of Gist feature extraction

On the other hand, our panoramic image is composed of 16 images of different directions to cover the 360-degree view of a scene. For different viewing directions, the scene structure could be very different and the statistics of detected edges and the texture representation are different. In Figure 3-11, we show the visualization of gist features in polar plots, where along the radius green and red colors are used to

represent different responses of multi-scale filters. Filter responses of different orientations are encoded in different angles of the polar plots. The brightness of the color represents the magnitude of the response. The 16 polar plots indicate the filter responses of the 16 non-overlapping local image regions. In Figure 3-11, we can easily distinguish the difference of gist feature among different images. In our system, the gist feature of each sub-image in the panoramas is pre-calculated to reduce the computation time. To measure the similarity between two images, we calculate the correlation of their corresponding gist features. If we denote  $p$  as the index of the 96 sub-images,  $X_p$  as the  $p$ th sub-image, and  $G(I)$  as the gist feature of the input frame, we find the best match  $X_p$  based on the following equation

$$X_p^* = \arg \min_{X_p} G(I)G(X_p)' \quad \text{Eq. 3-1}$$



*Figure 3-11 Visualization of Gist feature for different image views*

### 3.2.2. Spatio-temporal Constraint for Search Window

In our system, we assume that the blind user don't move drastically. That is, the panning speed and the walking speed are not too fast. With the slow motion assumption, the orientation of the matched sub-image at the current moment will be very similar to the orientation of the matched sub-image at the previous moment. As

shown in Figure 3-12, if the image portion between the red dash lines represents the best match for the previous input frame, then the orange region indicates the possible image portions for matching at the current moment. This assumption can greatly reduce the search range within the sub-database. In mathematics, this concept can be modeled as a Markov chain, as expressed in Equation 3-2. Here,  $\Pr(X_t = i)$  denotes the probability at Time  $t$  that the best matched image portion is the  $i$ th sub-image in the sub-database.

$$\Pr(X_t = j) = p_{r,j} \Pr(X_{t-1} = r) \quad \text{Eq. 3-2}$$

where  $p_{ij} = \Pr(X_t = j | X_{t-1} = r) \quad \text{Eq. 3-3}$

For the implementation detail, we search for the 7 nearest directions out of all 32 directions based on the direction of the previous best match. After global feature matching, we obtain the current facing direction of the user. The matched portion of the panoramic image also roughly interprets the surrounding environment.

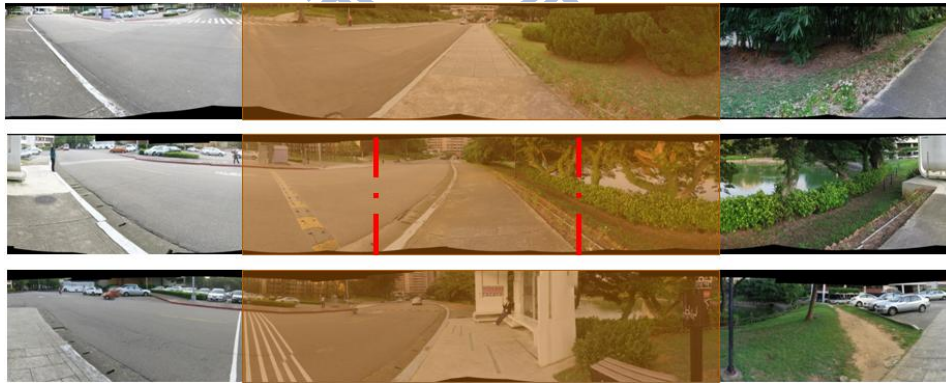


**Figure 3-12** Slow motion of blind user reduces the search area within the panoramic images.

### 3.3. SCENE ALIGNMENT AND LABEL

## TRANSFORMATION

As mentioned above, we have found the image portion of the panoramic images in the sub-database that is the most similar to the front view of the blind user. Here, we call this best matched image portion as the reference image of the input frame. As a matter of fact, there still exist some differences between the input frame and the best match, as shown in Figure 3-13. That is, even though these two images are captured at similar places with similar facing directions, the scene contents are not exactly the same. Hence, we need to further align the best match with the input frame to obtain more accurate labeling results.



*Figure 3-13 (a) Input frame. (b) The best matched image portion.*

For the sake of mapping the best match to the input frame, we focus on finding the correspondence between the two images. Up to now, many state-of-the-art methods have discussed this correspondence problem. One approach is to find some interest points of the images for matching, such as SIFT feature points. However, this sparse approach tends to have poor results when there are no appropriate interest points in the images. Another approach is to use the correspondence of regions to match the images, such as the approach in [19]. In this kind approach, they first

segment the images into many sub-regions. After that, they use some suitable features of the sub-regions to match the images. Intuitively, the matching result will be not accurate if the sub-regions are not accurately segmented.

In our approach, we adopt pixel-wise matching. Although the result of pixel-level matching is usually noisy, we can utilize some robust feature to tackle this problem. Here, we use SIFT flow proposed in [20] to perform pixel-wise matching in order to obtain better scene alignment.

### 3.3.1. SIFT Flow

SIFT flow is a novel method for the application of scene alignment. It adopts the same computational framework of optical flow to achieve dense matching. Instead of using RGB values and gradient information to represent the pixels, SIFT flow uses pixel-wise SIFT feature instead. Since this kind of histogram-based features contains contextual information around the pixel, we can use them to obtain more reliable matching results across different scene appearances. Moreover, the SIFT descriptor performs well under luminance variations of outdoor environment.

To better observe the generation of SIFT feature map, we adopt the visualization method shown in Figure 3-14. In this representation, after principal component analysis (PCA), the top three principal components of the 128-dimensional SIFT descriptors are calculated and are projected into the RGB space for visualization. In Figure 3-14, pixels with similar colors would share similar local image structure.

Even though we only use the top three principal components of the SIFT features for visualization, we use the 128-dimensional SIFT descriptors for dense matching. The objective function of the matching process is expressed as below:

$$E(\mathbf{w}) = \sum_{\mathbf{p}} \min(\|s_1(\mathbf{p}) - s_2(\mathbf{p} + \mathbf{w}(\mathbf{p}))\|_1, t) + \sum_{\mathbf{p}} \eta(|u(\mathbf{p})| + |v(\mathbf{p})|) + \sum_{(\mathbf{p}, \mathbf{q})} \min(\alpha |u(\mathbf{p}) - u(\mathbf{q})|, d) + \min(\alpha |v(\mathbf{p}) - v(\mathbf{q})|, d) \quad \text{Eq. 3-4}$$

Here,  $\mathbf{p}$  and  $\mathbf{q}$  are pixel coordinates. The notation  $s$  indicates the SIFT image and  $\mathbf{w}$  indicates the flow vectors. The first term in Equation 3-4 is the feature matching term, also known as the data term. In this term, SIFT features are matched across the two images. The second term sets a constraint that the flow magnitude should not be too large, with  $\eta$  representing the weighting of this constraint. The third term models the spatial regularization so that the flow vectors of adjacent pixels will be similar, with  $\alpha$  representing the coefficient of flow discontinuity. The dual-layer loopy belief propagation [21] is adopted to obtain the optimized flow field, which allows the separation of the vertical flow from the horizontal flow in message passing by decoupling the smoothness term.

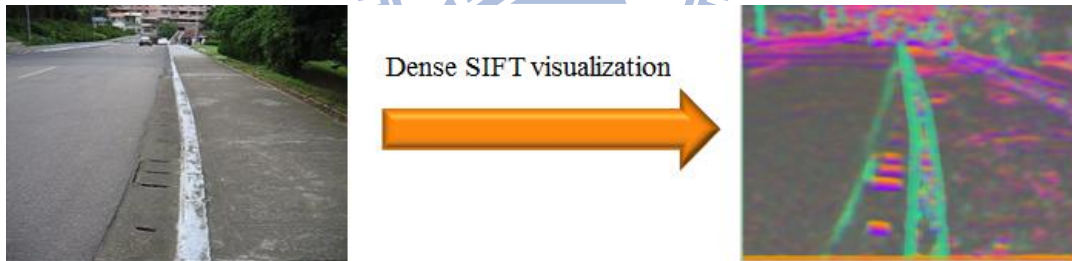


**Figure 3-14** Visualization of SIFT features

After the optimization process, we obtain the SIFT flow field. Based on the flow vectors, we can warp the pixels of the best matched image for image alignment. As shown in Figure 3-15, the warped image will be quite similar to the input image frame.



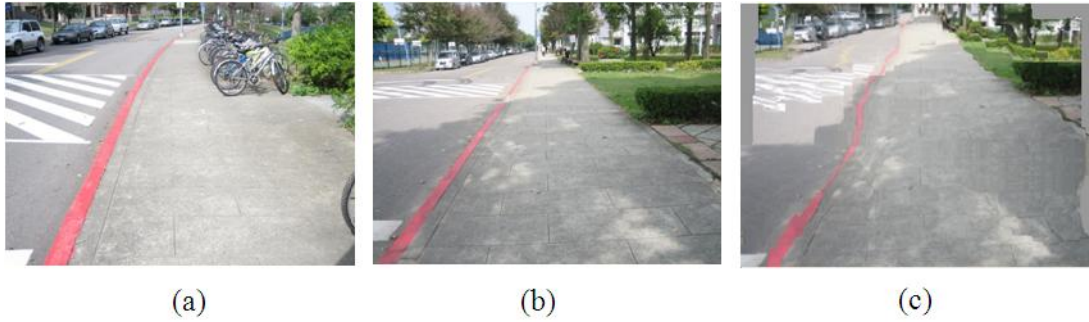


**Figure 3-15** (a) Input frame. (b) Best match from database. (c) Warped image.

Similarly, we map the labels of the best matched image along the flow vectors. The mapped label can be taken as the inference of the environment, as shown in Figure 3-16, where the green labels represent the sidewalk area and the red labels represent the road area. To keep the completeness of region and to suppress some outliers, we actually have performed the morphological “open” operation after the mapping of labels.

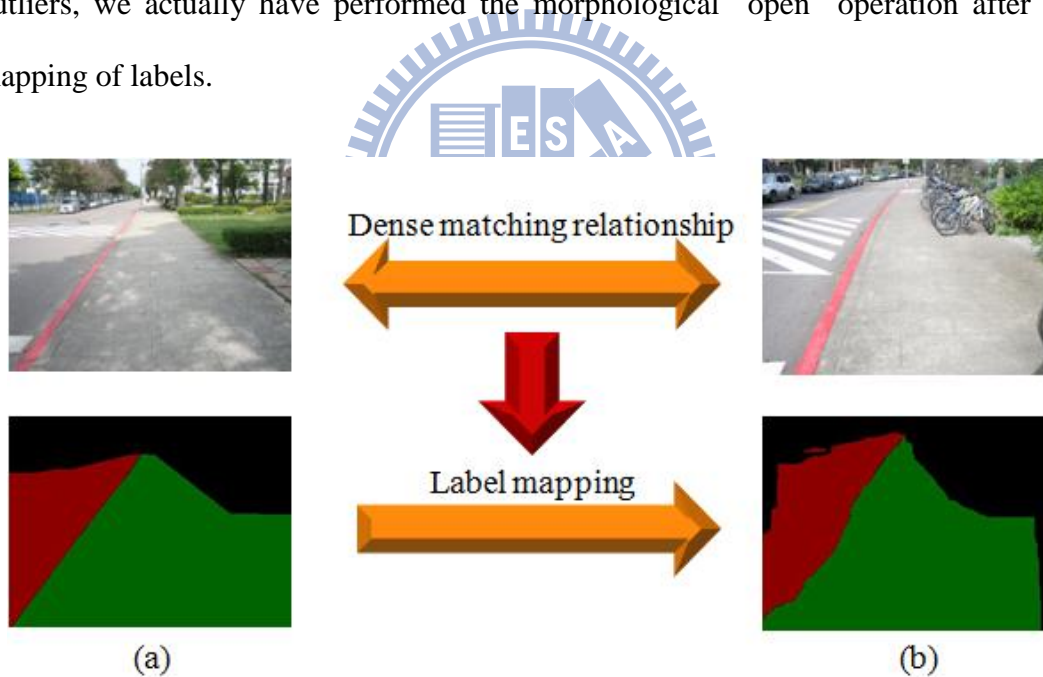


**Figure 3-16** (a) Best match and the corresponding labels.

(b) Input frame and the inferred labels.

As mentioned above, based on pixel-wise matching, we can map the labels of the best matched image to interpret the contents of the input image frame. The reasons why we don’t use optical flow for dense correspondence are as follows. First, the assumption for optical flow doesn’t fit our problem. Most optical flow methods are



used to describe the temporal correspondence of two successive frames in a video sequence. Due to the significant similarity between two successive frames, the assumption of consistent brightness is usually used and a small search window is usually adopted. For our case, however, there always remains certain appearance difference between the best matched image and the input frame. Hence, the traditional optical flow method may not be appropriate for our situation. Moreover, the SIFT flow approach utilizes a larger search window so that we can tolerate larger differences between these two images in scene alignment, as shown in Figure 3-17.

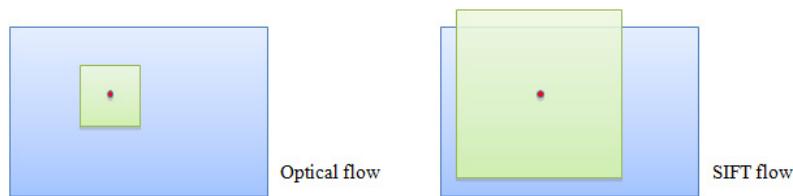


**Figure 3-17** Different size of search window for optical flow and SIFT flow

To build meaningful correspondence between two images, we assume that these two images share a similar local image structure. The perspectives of the images are also assumed to be similar. However, the blind user may have various kinds of movement while walking on the sidewalk, such as a horizontal move shown in Figure 3-18. Under this example, the SIFT flow may not be able to perform meaningful correspondence due to the different perspective caused by the horizontal move.



**Figure 3-18** Illustration of poor alignment. (a) Input frame. (b) Best match. (c) Warped image.

In the above example, even though these two images are taken at the same place, we still can't obtain a convincing flow field to represent the matching relation. Because of the insufficient information provided by a single support image, the mapped image is not very similar to the input frame.

### 3.3.2. Panoramic Approach

To provide a more accurate warping result, instead of taking a single support image for dense matching, we utilize a larger image portion in the panoramic image, as shown in Figure 3-19. The extended support image is about 2.5 times wider than the width of the input frame, but with the same height. Moreover, to search over a wider support image, we also relax the constraint of flow magnitude. The weighting of flow constraint is set to 0.4 times of the original setup. With the extended support image and the relaxed flow magnitude constraint, more panoramic information can be acquired for better dense matching, as shown in Figure 3-20.

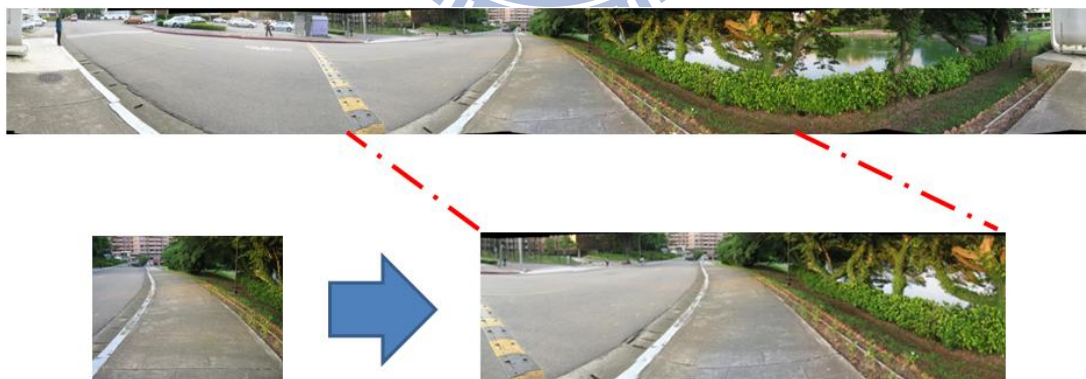


*Figure 3-19 Panoramic extension of the original support image.*

2.5 times wider !

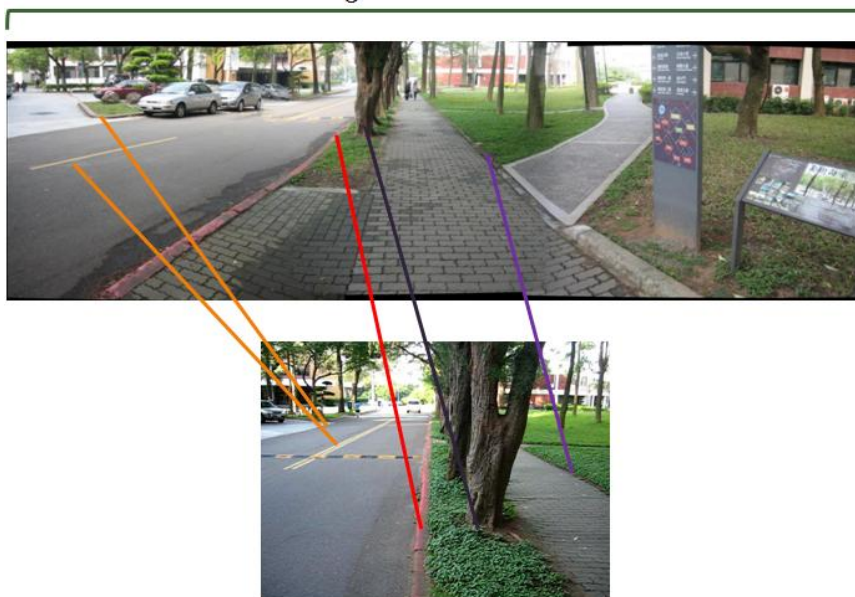


*Figure 3-20 More information is acquired by using panoramic approach.*

*Top: extended support image. Bottom: input frame.*

*Color lines indicate feature correspondence*

## 3.4. DANGEROUS SITUATION DETECTION

By using the inferred labels, we can decide whether the situation in front of the blind user is dangerous or not. Here we focus on the relation between road and sidewalk and apply a rule-based method to analyze these labels. Since humans typically pay more attention to the central region in front of them, we define the region of interest to be the trapezoid mask shown in Figure 3-21.



*Figure 3-21 Region of interest that models human's visual attention area.*

The complete flow diagram of dangerous situation detection is illustrated in Figure 3-23. The first dangerous situation is defined to be the case when the road

region is larger than the sidewalk region in the trapezoid mask. This situation usually occurs when the user turns his/her direction toward the road or when the user's position is near the border between road and sidewalk. Here, we define the area of road label inside the mask as  $A_r$  and the area of sidewalk label as  $A_s$ . As expressed in Equation 3-5, when the area ratio  $A_{ratio1} = A_r/A_s$  is larger than a certain threshold  $Th_{area1}$ , we infer the situation as dangerous. In our system,  $Th_{area1}$  is empirically set to 0.325.

On the other hand, the blind user may walk to the border between the sidewalk and some region other than road. For this case, we denote the unlabeled region as "undefined" and denote its area as  $A_{un}$ . As expressed in Equation 3-5, when the ratio  $A_{ratio2} = A_{un}/A_s$  is larger than another threshold  $Th_{area2}$ , we infer that situation to be dangerous too. In our system, the threshold  $Th_{area2}$  is empirically set to 0.8.

$$\begin{cases} D_1=1, \text{ if } A_{ratio1} = \frac{A_r}{A_s} > Th_{area1} \\ D_1=1, \text{ if } A_{ratio2} = \frac{A_{un}}{A_s} > Th_{area2} \\ D_1=0, \text{ otherwise} \end{cases} \quad \text{Eq. 3-5}$$

After analyzing the area ratio of different labels, we check whether the sidewalk region is right in front of the user. In other words, even if the area ratios are lower than corresponding threshold, the situation would be dangerous if there is no sidewalk label at the bottom of the trapezoid mask. Here, we infer the situation as dangerous if there is no sidewalk label within the bottom 15% region of the trapezoid mask. Here, we denote this bottom 15% region as  $M_b$ , as expressed in Equation 3-6.

$$\begin{cases} D_2 = 1, \text{ if } A_s = 0 \text{ in } M_b \text{ \& } D_1 = 0 \\ D_2 = 0, \text{ otherwise but } D_1 = 0 \end{cases} \quad \text{Eq. 3-6}$$

The other dangerous situation happens when the sidewalk area in front of the user is too small. Here, we detect this situation if the area of sidewalk label in the mask is under a certain rate  $R_s$ , as expressed in Equation 3-7. We define  $A_T$  as the area of trapezoid mask. In our system,  $R_s$  is empirically set to be 0.25.









$$\begin{cases} D_3 = 1, \text{ if } A_s < R_s \times A_T \text{ \& } D_2 = 0 \\ D_3 = 0, \text{ otherwise but } D_2 = 0 \end{cases} \quad \text{Eq. 3-7}$$

Hence, we detect the situation is dangerous if  $D_1$ ,  $D_2$ , or  $D_3$  is one. Otherwise, the situation is safe. After analyzing the label, the system can pass the message to the blind user so that he/she can know whether his/her current situation is dangerous or not. In real implementation, one can use an audio device to warn the blind user if he/she has the normal sense of hearing.

In addition to the detection of the dangerous situations for blind people, our system can also suggest the blind user the right direction of safe walking. After a dangerous situation is detected, we analyze the spatial layout of the warped labels to determine the right direction. In detail, we extract the pixel positions of each label class and average the coordinates of the horizontal component. If we define the center of the x coordinate of the road labels is  $C_r$  and the center of the x coordinate of the sidewalk labels is  $C_s$ , we can compare the values of  $C_r$  and  $C_s$  to determine the suggested turning direction. If there is no road label, we just check whether  $C_s$  is on the right half or on left half of an image. If the area of sidewalk labels is too small, the spatial layout of labels would be unreliable. In this case, we estimate the safe direction by using the label information at the previous moment. In Figure 3-22, we present the

pseudo code of the decision process.

```

if danger
  if area of sidewalk label > 0.25 * image width * image height
    then compare  $C_s$  &  $C_r$  of the input frame
    if there is road label
       $C_s < C_r$  : turn left 
       $C_s > C_r$  : turn right 
    else
       $C_s$  is smaller than half image width: turn left 
       $C_s$  is larger than half image width: turn right 
    endif
  endif
  else
    then compare  $C_s$  &  $C_r$  of the label of last safe situation
    if there was road label
       $C_s < C_r$  : turn left 
       $C_s > C_r$  : turn right 
    else
       $C_s$  was smaller than half image width: turn left 
       $C_s$  was larger than half image width: turn right 
    endif
  endif
endif

```

Figure 3-22 Decision rules for direction turning

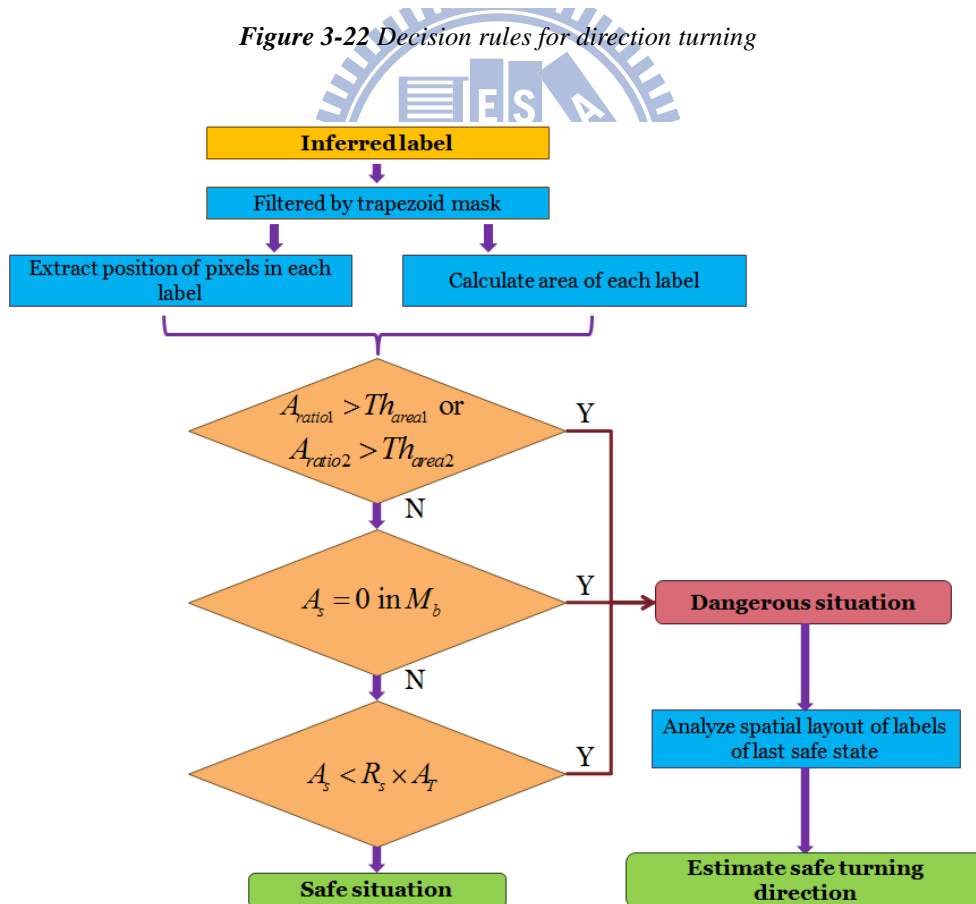


Figure 3-23 Flow diagram of dangerous situation detection

### 3.5. TEMPORAL INTERPOLATION

In order to reduce the computational complexity, another approach is to utilize temporal information. Instead of performing the whole process for every frame, we can use temporal correspondence to simplify the process. In our system, we perform the whole process only over a few frames, named the anchor frames. For each anchor frame, we perform sub-database retrieval and calculate SIFT flow to generate the outcome. For those frames between a pair of adjacent anchor frames, we simply propagate the labeling results of the anchor frame to estimate their labels. This process is illustrated in Figure 3-24 below.

On the other hand, the camera may pan when the blind user turns left or right, as shown in Figure 3-25. For this case, we track the camera status using the statistics of the SIFT flow between adjacent frames.

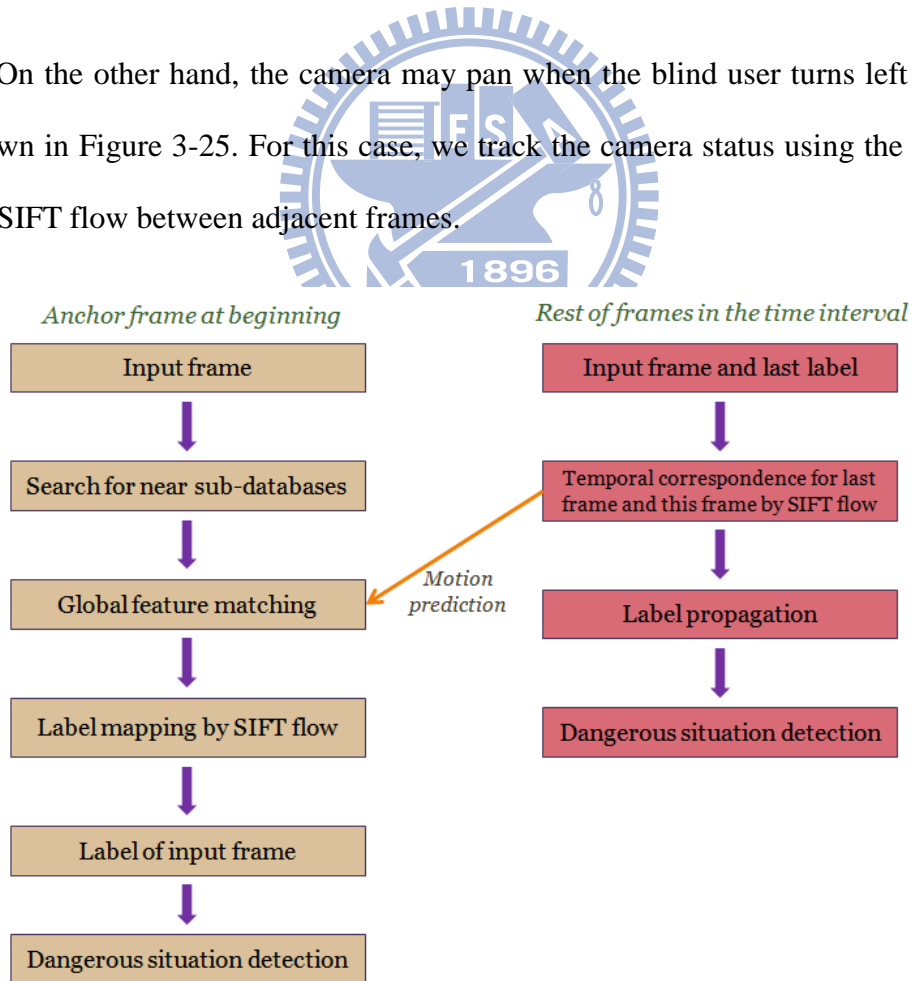


Figure 3-24 Simplified architecture by using temporal information.





*Figure 3-25 Camera panning caused by the turning of the user.*

### 3.5.1. Motion Prediction

As mentioned above, to deal with the panning of camera, we analyze the SIFT flow between two adjacent frames. Again, because of the larger search window used in the calculation of SIFT flow, we will be able to handle a large motion. To predict the motion, we analyze the flow field in the horizontal direction. Here, we calculate the mean of the flow magnitude along the horizontal direction. This result indicates the turning direction of the user. As shown in Figure 3-26 and Figure 3-27, we take the histogram of the flow magnitude in the horizontal direction. When the mean of the horizontal flow magnitudes is lower than  $-20$ , we infer the user as turning left. On the other hand, when the mean value is larger than  $20$ , we infer the user as turning right. Some examples are shown below in Figure 3-26 and Figure 3-27.

### 3.5.2. Label Propagation

As mentioned above, we use temporal information to propagate the labels for non-anchor frames. The labeling results of the preceding frame are warped to generate the labels of the current frame based on the temporal correspondence between these two frames. The use of temporal correspondence makes the labeling results reliable and accurate as long as we have obtained correct labels in the anchor frame.



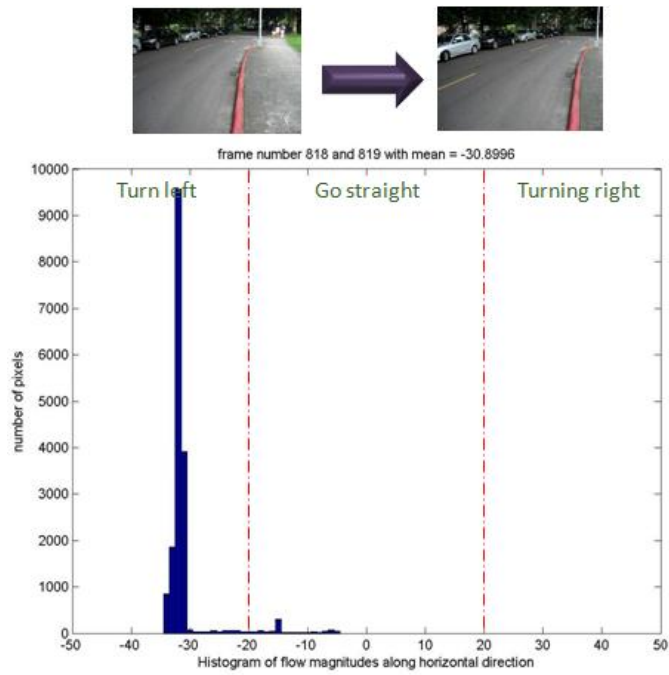


**Figure 3-26** Histogram of SIFT flow magnitudes in the horizontal direction when the user turns left. The green words indicate the inferred camera status.

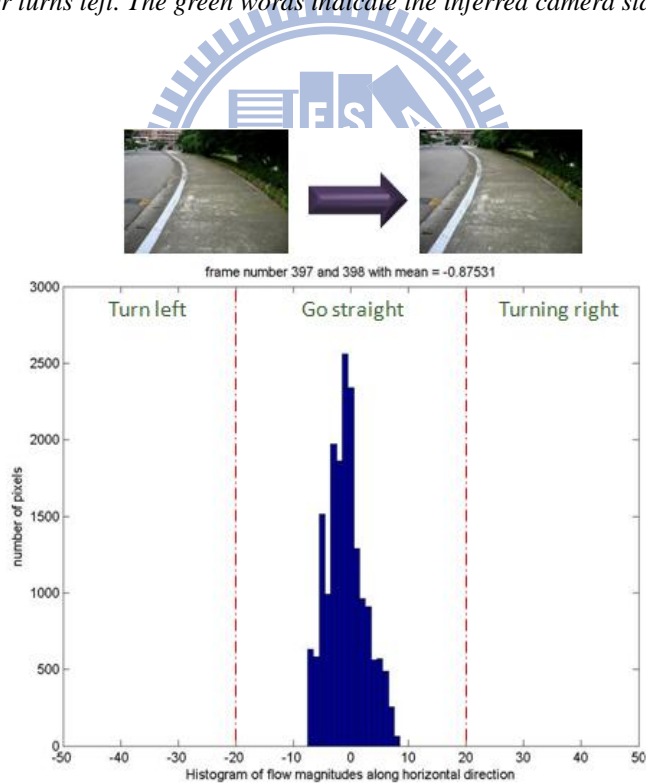


**Figure 3-27** Histogram of SIFT flow magnitudes in the horizontal direction when the user walks straight. The green words indicate the inferred camera status.

# Chapter 4.

## EXPERIMENTAL RESULTS

In this chapter, we will demonstrate some of our experimental results. In Section 4-1, we will show the results of label transformation by the SIFT flow with single view approach and by the SIFT flow with panoramic approach. In Section 4-2, we will show the performance of our system over a real outdoor environment in NCTU. Our proposed system is tested over a personal computer with Intel® Core™ i5-760 CPU at 2.8G Hz. Our algorithm is developed in Matlab but without code optimization.

### 4.1. LABEL RESULTS OF DIFFERENT APPROACHES



First, we show the warping and label results by SIFT flow with the single-view approach and with the panoramic approach. A result is shown in Figure 4-1, which shows that the panoramic approach provides more accurate warping and label result. The parameters of SIFT flow are set to be the same for both cases. The input frame is captured at the resolution of 640×480 pixels and then down-sampled to 160×120 pixels. The panoramic image is 2.5 times wider than the input frame, but with the same height.

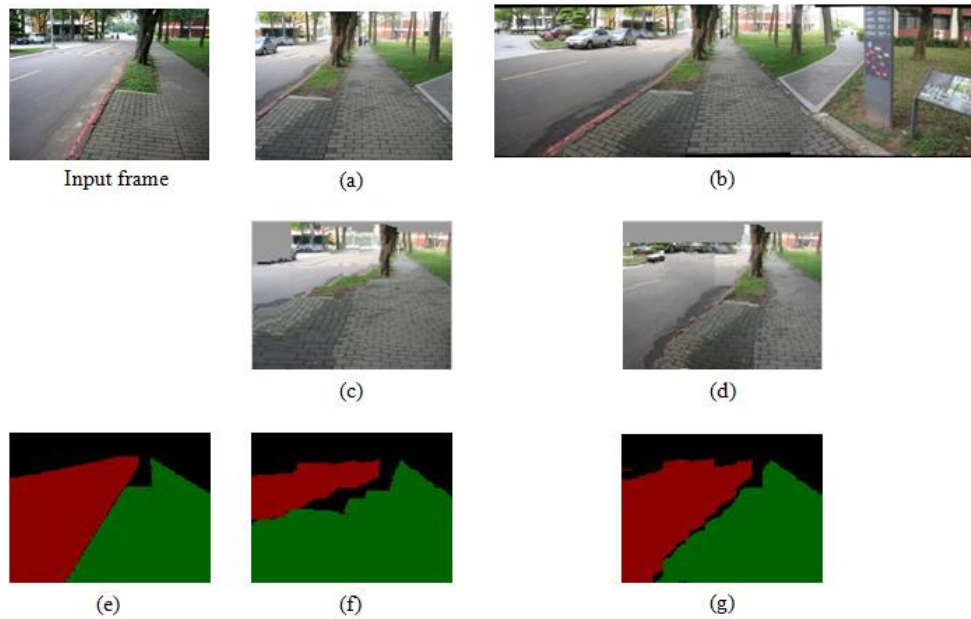


**Figure 4-1** (a) Single-view support image, (b) panoramic-view support image, (c) warped result from single-view image, (d) warped result from panoramic-view image, (e) ground truth labels, (f) mapped labels based on single-view support, and (g) mapped labels based on panoramic view.

Another example is shown in Figure 4-2. Via panoramic approach, even though the results of warped image and label do not perfectly resemble the input frame, the results can still well represent the input frame.

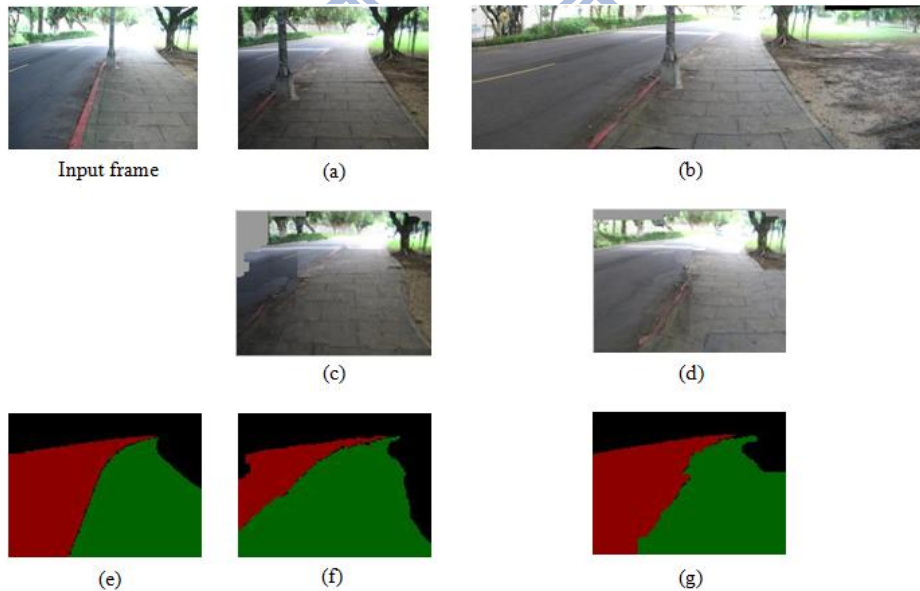


**Figure 4-2** (a) Single-view support image, (b) panoramic-view support image, (c) warped result from single-view image, (d) warped result from panoramic-view image, (e) ground truth labels, (f) mapped labels based on single-view support, and (g) mapped labels based on panoramic view.

## 4.2. OUTDOOR EXPERIMENTAL RESULTS

### WITHIN NCTU

#### 4.2.1. Database Setup

Our system is tested on two routes near the north gate of National Chiao Tung University (NCTU), as shown in Figure 4-3. Red lines indicate these two routes, which consist of various kinds of scenes, such as bus station, intersection, or trees, as shown in Figure 4-4. The total length for these two routes is about 300 meters.



*Figure 4-3 Our test routes in NCTU.*



*Figure 4-4 Scene appearances*

To create the database along these two routes, we choose 11 sampling spots in total. The selection of sampling spots is based on three criteria: 1) a scene that contains an intersection, 2) a scene that contains informative landmarks, such as crosswalk and waymark, and 3) a scene that contains special construction, like bus station. We follow these criteria to build our panoramic database. As aforementioned in Section 3-1-1, we take 16 photographs of different views at each sampling spot to create the panoramic image.

## 4.2.2. Experimental Results in Test Environments

We test our system over three video sequences that were captured in three different weather conditions: cloudy days, sunny days with some unexpected shadows in the scene, and evening time with low lighting condition. Here we show some inferred label and detected dangerous situations. The resolution of the videos is 640×480. The test procedure of our system includes the panoramic approach and temporal interpolation mentioned in Section 3.3.2 and Section 3.5. The test video of the sunny situation was captured around 14:00 in the afternoon, while evening video was captured around 18:00 in the evening. While taking these video sequences, we mimicked the way blind people take a straight walk until the ‘real’ dangerous situation occurs. Hence, the walking tracks follow a zigzag style. We sample all the test video with the sampling period of 0.6 seconds. For every 6 seconds, we pick an anchor frame. In our experiments, the detection process is performed over the anchor frames only. For the remaining frames between anchor frames, we use temporal information to propagate labels.

### 4.2.2.1. Results of Database Retrieval

In Section 3-2, we have discussed how to find the portion of panoramas which is most similar to the sight in front of the blind user. Here we show some examples of the best matches after sub-database retrieval by using gist feature matching with the spatio-temporal constraint.



**Figure 4-5** Results of database retrieval for walking forward with some pedestrians passing by. (a) Frame index, (b) input frames, and (c) the best match from the panoramic sub-database.

In the previous example, we can see that the interference in the local image structure, such as passing pedestrians, doesn't affect the outcome of database retrieval too much. The best matched part and input frame would share a similar local structure. In comparison, in the following example, we show the case of a panning view.

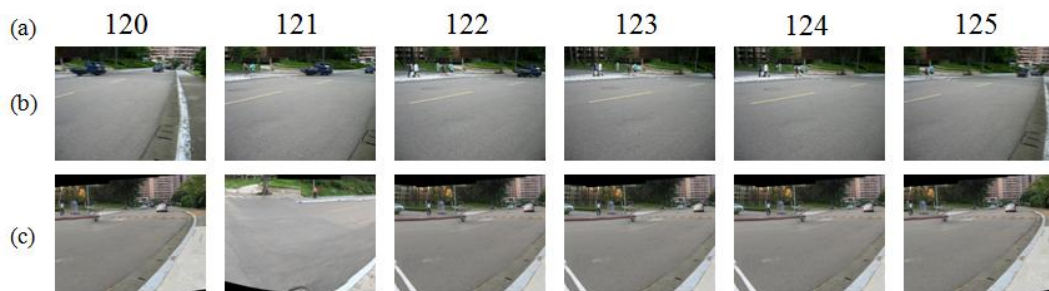


**Figure 4-6** Results of database retrieval for a panning case. (a) Frame index, (b) input frames, and (c) the best match from the panoramic sub-database.

### 4.2.2.2. Cloudy Day

For the test video captured in a cloudy day, its lighting condition is very similar to that in our database. Some results of the cloudy-day case are shown below. Here, we show different walking situations on the sidewalk and the detected dangerous situations. To visualize the outcome of our system, we use an exclamation mark to represent the occurrence of dangerous situation. Moreover, the yellow arrow indicates the suggested safe way to turn if a danger situation is detected. The case of walking forward is shown in Figure 4-7.

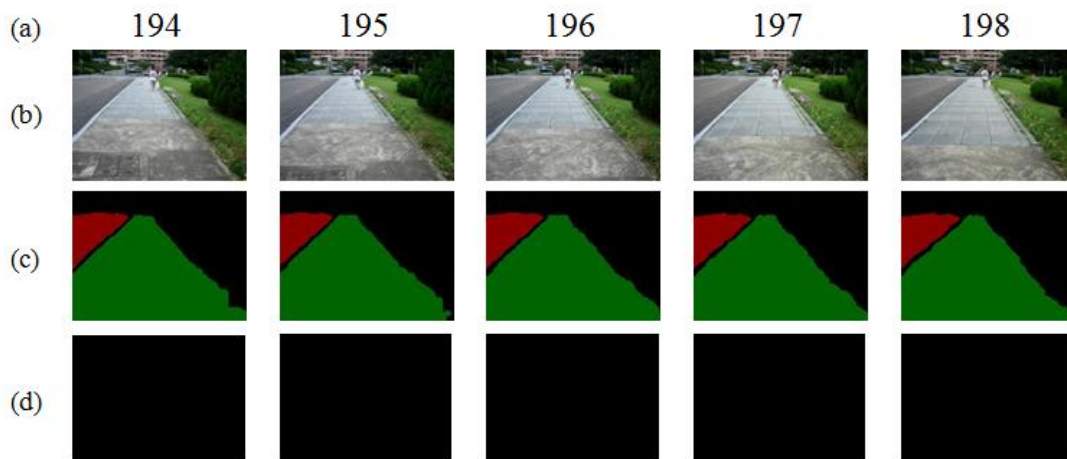


**Figure 4-7** The case of walking forward in safe situation. (a) Frame index. (b) Input frames. (c) Inferred labels. (d) Outcome of dangerous situation detection.

Next, we show an example in which the blind user turn into a wrong direction. In this case, our system will warn the user the detection of a dangerous situation. In this example, the system informs the user to turn right to achieve safe walk.



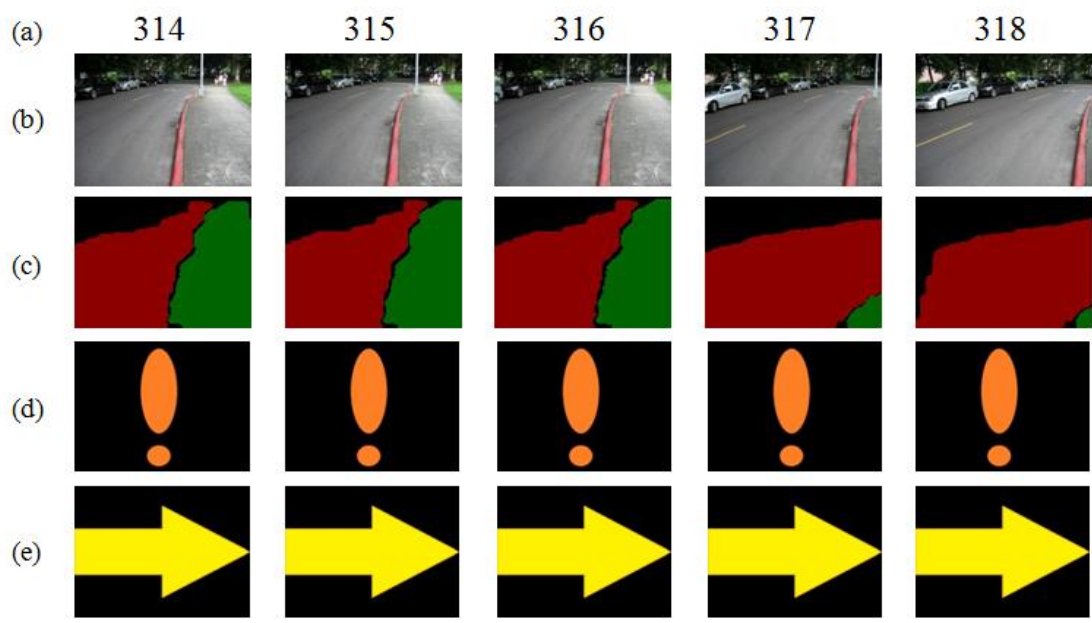


**Figure 4-8** The case of turning to a wrong direction. (a) Frame index. (b) Input frame. (c) Inferred labels. (d) Outcomes of dangerous situation detection. (e) Suggested turning direction.

In the previous example, we still find that the labels are not perfectly accurate for Frames 317 and 318. However, the tendency of the change of mapped labels along the temporal domain is correct. That is to say, the result of dangerous situation detection is still correct even if the labels are not perfectly correct. For Frames 314~316, one could see that the user walks on the sidewalk border. We also treat this situation as dangerous. One more dangerous situation occurs when the blind user walks on the border of sidewalk and road. In this case, our system detects the occurrence of dangerous situation and suggests the blind user turn right for safe walk.



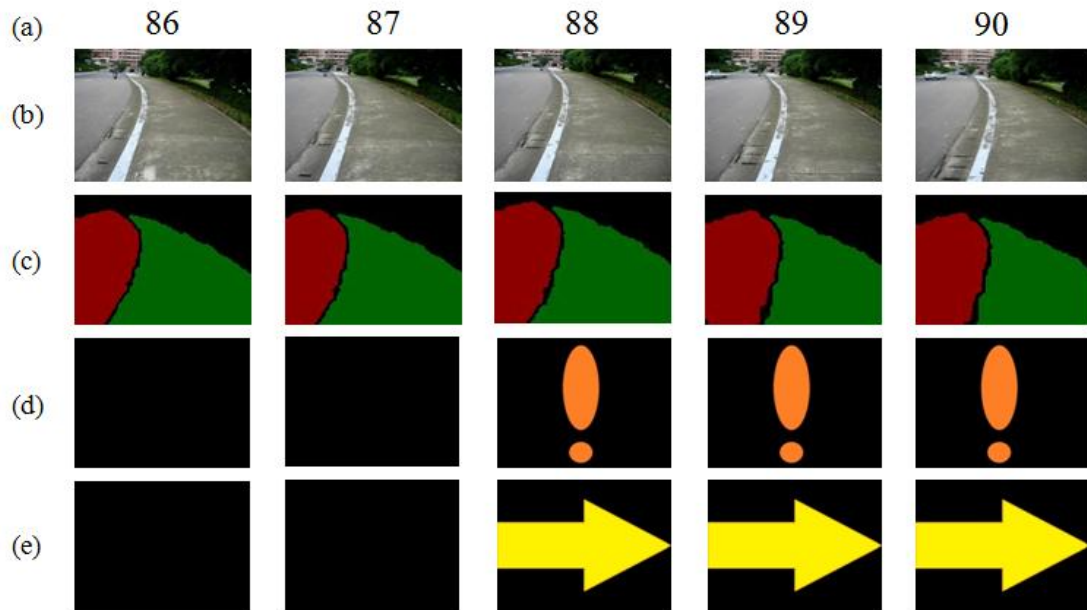


**Figure 4-9** The case of approaching to the border of sidewalk and road. (a) Frame index. (b) Input frame. (c) Inferred labels. (d) Outcome of dangerous situation detection. (e) Suggested turning direction.

The final example in figure 4-10 shows the dangerous situation when there is little sidewalk area in front of the blind user.

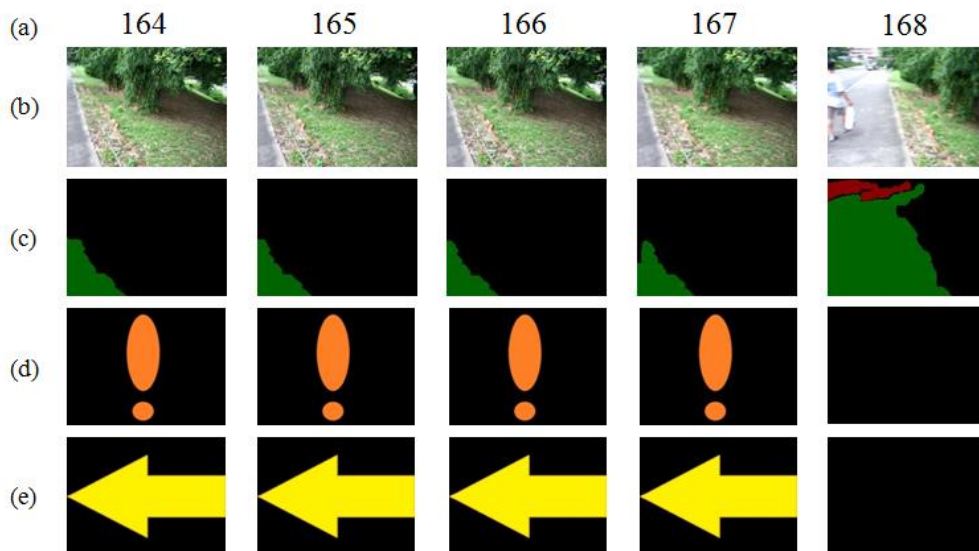


**Figure 4-10** The case of little sidewalk area in front of the user. (a) Frame index. (b) Input frame. (c) Inferred labels. (d) Outcome of dangerous situation detection. (e) Suggested turning direction.

### 4.2.2.3. Sunny Day and Evening Time

For sunny days, the shades projected on the objects usually cause difficulty in detection and recognition. Due to the strong edges caused by shadows, the processes of sub-database retrieval and label mapping may easily get affected. On the other hand, the lighting condition is usually poor for outdoor environment during the evening time. In the following examples, we show the performance of our system under these two weather conditions.



**Figure 4-11** Test results in sunny day. (a) Input frames. (b) Inferred label. (c) Outcome of dangerous situation detection. (d) Suggested turning direction.

The above figure shows some simulation results for the test video captured in a sunny day. The performance of our system is not too bad under slight shadow interference. However, for the rightmost frame in Figure 4-11, there is a huge dark area in front of the user caused by the shade of tree. In this case, our system may infer incorrect labels.

In the following case, we show the simulation results at evening time. In some

scenes, the light condition is very poor, such as these places near trees. In this kind of poor lighting condition, our system may not generate correct outcome.



**Figure 4-12** Some examples at evening time. (a) Input frame. (b) Inferred labels. (c) Outcome of dangerous situation detection. (d) Suggested turning direction.

#### 4.2.2.4. Experimental Data

First we analyze the accuracy of sub-database retrieval. We recall that each panorama in the sub-database is partitioned into 32 overlapping parts, representing 32 viewing directions. For the accuracy of sub-database retrieval, we define the best match is accurate if its corresponding direction is within the 4 nearest directions of the user's true facing direction. We test the accuracy of sub-database retrieval using the aforementioned three videos. In the cloudy-day video, we test 438 frames to measure the accuracy. In sunny-day and evening-time videos, we test 385 and 425 frames, respectively.

**Table 4-1** Accuracy of sub-database retrieval

	Cloudy	Sunny	Evening
Accuracy (%)	97.717	97.143	94.479

When analyzing the experimental outcome of our system, we regard our issue as

a detection problem. We take the detected dangerous situation as the positive outcome. The definitions of false positive and false negative are listed in Table 4-2.

**Table 4-2** Definition of false positive and false negative

	True dangerous situation	True safe situation
System detects dangerous situation	True positive	False positive
System detects safe situation	False negative	True negative

The equations for detection rate, false positive rate, and false negative rate are defined as below:

$$\text{Detection rate} = \frac{\text{true positive} + \text{true negative}}{\text{total numbers of sampled frames}} \quad \text{Eq. 4-1}$$

$$\text{False positive rate} = \frac{\text{false positive}}{\text{false positive} + \text{true negative}} \quad \text{Eq. 4-2}$$

$$\text{False negative rate} = \frac{\text{false negative}}{\text{false negative} + \text{true positive}} \quad \text{Eq. 4-3}$$

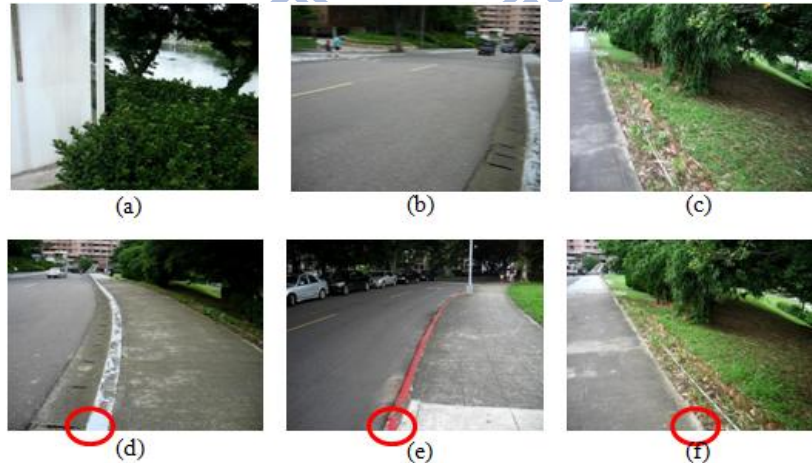


**Figure 4-13** Ground truth definition (a) to (c): apparent cases, (d) to (f): use the location of border to determine whether it is a dangerous situation.

For the case of cloudy days, we test our algorithm over 438 images, in which 110 images indicate dangerous situations. By comparing our panoramic approach with temporal information to the single-view approach, we can see that the panoramic

approach is more reliable. In the test of the single-view approach, we create a database which is composed of 8 single-view images representing 8 different viewing directions at each sampling spot. For the spatio-temporal constraint, we search for 3 nearest facing directions of all 8 directions based on the best match at the previous moment. Other procedures are set to be the same as the panoramic approach. The cases of walking to the border between sidewalk and road (shown in Figure 4-9) are not detected as a dangerous situation by the single-view approach. The ground truth results are defined manually. Some dangerous cases are quite apparent. However, for the case of approaching to the border of sidewalk, we use the position of border to determine whether it is a dangerous situation. If the border of sidewalk at the bottom of the image locates within the central one third of the image width, we define the situation to be dangerous, as shown in Figure 4-13.

**Table 4-3** Experimental data at cloudy day and comparison of single-view approach

	Detection rate (%)	False positive rate (%)	False negative rate (%)
Panoramic approach	95.205	3.354	9.091
Single-view approach	77.854	9.756	59.091

For the evening-time case, we test our system over 425 images, in which 77 images indicate dangerous situations. For the sunny-day case, we test over 385 images, in which 79 images indicate dangerous situation.

**Table 4-4** Experimental data under different lighting conditions

	Detection rate (%)	False positive rate (%)	False negative rate (%)
Sunny	92.727	5.882	12.658
Evening	93.381	3.736	22.078

In the above simulations, false positives and false negatives usually occur in some frames right before or right after the frames of dangerous situations. This

phenomenon tells us that our system may be able to detect the situation when the user “really” approaches dangers.

The computing time of our algorithm is listed in Table 4-5. When we take the full procedure starting from sub-database retrieval to the detection of dangerous situations, the computation time is about 4.25 seconds. By using temporal information, we only need three seconds per frame for non-anchor frames. The three seconds are almost spent by the computation of SIFT flow. We recall that the resolution of the test videos is 640×480. When using SIFT flow to achieve scene alignment, we don’t need to use the full image resolution. Instead, the width and height of the input frame and the support image are down-sampled to 0.25 times of the original images. Because the numbers of nodes are reduced to 1/16 for belief propagation, the computation time is much faster, while still maintaining similar performance in label mapping.

*Table 4-5 Computational speed for our system*

	Full procedure	Using temporal information (anchor frame)	Using temporal information (remaining frames)
Process time per frame (seconds)	4.25	4.25	3.065

# Chapter 5.

## CONCLUSIONS

In this thesis, we propose a vision-based travel aid system for blind people. Our system can label the walking area in front of the blind user and automatically detect the occurrence of dangerous situation. With the proposed system, blind user can know which direction would be safer to walk along. In our system, we adopt a database-driven framework. First we utilize blind user's position coordinate and gist feature to find a part of panoramas which is the similar to the view in front of the user. After that, we exploit the SIFT flow for image alignment. We map the label of the best matched sub-image to infer the labels of the input frame. Finally we use the label information to detect the dangerous situation. Our system is able to run on different kinds of environments as long as the local database is installed beforehand. Some experimental results have shown our system is reliable under different weather conditions.



# REFERENCES

- [1] D. Dakopoulos, and N. G. Bourbakis, "Wearable Obstacle Avoidance Electronics Travel Aids for Blind: A Survey," *IEEETransaction on Systems,Man, and Cybernetics, Part C: Applications and Reviews*, vol. 40, no. 1, pp. 25-35, Jan. 2010.
- [2] S. Shoval, J.Borenstein, and Y.Koren, "The Navbelt-A Computerized Travel Aid for the Blind Based on Mobile Robotics Technology," *IEEETransactions on Biomedical Engineering*, vol. 45, no. 11, pp. 1376-1386, Nov.1998.
- [3] J. Borenstein, and I. Ulrich, "The GuideCane-A Computerized Travel Aid for the Active Guidance of Blind Pedestrians," in Proc. *IEEE International Conference on Roboticsand Automation*, vol. 2, Albuquerque, NM, USA, Apr 1997, pp. 1283-1288.
- [4] J. M. Benjamin, N. A. Ali, and A. F. Schepis, "A Laser Cane for the Blind," *IEEE Journal of Quantum Electronics*, vol. 3, pp. 268, Jun. 1967.
- [5] D. Yuan, and R. Manduchi, "A Tool for Range Sensing and Environment Discovery for the Blind," *IEEE Conference on Computer Vision and Pattern RecognitionWorkshop*,pp. 39-39, Jun. 2004.
- [6] D. Yuan, and R. Manduchi, "Dynamic Environment Exploration Using a Virtual White Cane," *IEEE Conference on Computer Vision and Pattern Recognition*,vol. 1, pp. 243-249, Jun. 2005.
- [7] B. Ding, H. Yuan, L. Jiang, and X. Zang, "The Research on Blind Navigation System Based on RFID", *IEEE International Conference on Wireless Communications, Networking and Mobile Computing*, , Shanghai, China, Sept 2007.
- [8] João José, M. Farrajota, João M.F. Rodrigues, J.M. Hans du Buf, "The Smart Vision Local Navigation Aid for Blind and Visually Impaired Persons," *International Journal of Digital Content Technology and its Applications*, Vol.5 No.5, May 2011.
- [9] J. Lafferty, A. McCallum, and F. Pereira, "Conditional Random Fields: Probabilistic Models for Segmenting and Labeling Sequence Data," in Proc. *International Conference on Machine Learning*, pp. 282-289, 2001.
- [10] J.Shotton, J. Winn, C. Rother, and A. Crimini, "TextonBoost for Image Understanding: Multi-class Object Recognition and Segmentation by Jointly Modeling Texture, Layout, and Context," *International Journal of Computer Vision*, vol. 81, no. 1, pp. 2-23, Jan. 2009.
- [11] J. Tighe, and S. Lazebnik, "SuperParsing: Scalable Nonparametric Image Parsing



- with Superpixels,” *European Conference on Computer Vision, ECCV’10*, vol. 6315, Heraklion, Crete, Greece, pp. 352-365, Sep. 2010.
- [12] V. Paradeep, G. Medioni, and J. Weiland, “Robot Vision for the Visually Impaired,” *IEEE Computer Society Conference on Computer Vision and Pattern Recognition Workshops, CVPRW’10*, San Francisco, CA, pp. 15-22, Jun. 2010.
- [13] J. J. Liu, C. Philips, and K. Daniilidis, “Video-Based Localization Without 3D Mapping for the Visually Impaired,” *IEEE Computer Society Conference on Computer Vision and Pattern Recognition Workshops, CVPRW’10*, San Francisco, CA, pp. 23-30, Jun. 2010.
- [14] H. Bay, A. Ess, T. Tuytelaars and L. V. Gool, “SURF: Speeded Up Robust Feature,” *Computer Vision and Image Understanding, CVIU’08*, vol. 110, no. 3, pp. 346-359, Jun. 2008.
- [15] A. Oliva, A. Torralba, “Modeling the shape of the scene: a holistic representation of the spatial envelope,” *International Journal of Computer Vision*, vol. 42, no. 3, pp. 145-175, May. 2001.
- [16] B. C. Russell, A. Torralba, K. P. Murphy, W. T. Freeman, “LabelMe: a database and web-based tool for image annotation,” *International Journal of Computer Vision*, vol. 77, no. 1-3, pp. 157-173, May. 2008.
- [17] J. Hays, and A. A. Efros, “IM2GPS: Estimating Geographic Information from a Single Image,” *Proceedings of the IEEE Conf. on Computer Vision and Pattern Recognition, CVPR’08*, pp. 1-8, Jun. 2008.
- [18] A. Torralba, M. S. Castelano, A. Oliva and J. M. Henderson, “Contextual Guidance of Eye Movements and Attention in Real-World Scenes: The Role of Global Features,” *Psychology Review*, vol. 113, no. 4, pp. 766-786, Oct. 2006.
- [19] H. Zhang, J. Xiao, and L. Quan, “Supervised Label Transfer for Semantic Segmentation of Street Scenes,” *European Conference on Computer Vision, ECCV’10*, vol. 6315, Heraklion, Crete, Greece, pp. 561-574, Sep. 2010.
- [20] C. Liu, J. Yuen and A. Torralba. “SIFT flow: dense correspondence across different scenes and its applications.” *IEEE Transactions on Pattern Analysis and Machine Intelligence (TPAMI)*, vol. 33, no.5, pp. 978-994, May. 2011.
- [21] A. Shekhovtsov, I. Kovtun, and V. Hlavac, “Efficient MRF Deformation Model for Non-rigid Image Matching,” *Proceedings of the IEEE Conf. on Computer Vision and Pattern Recognition, CVPR’07*, pp. 1-6, Jun. 2007.